

A DELAYED FEEDBACK BASED PRACTICAL CHAOS CONTROL METHOD:  
TAIL APERTURE FEEDBACK

by

Dilge Terbaş

B.S., Electrical and Electronics Engineering, Middle East Technical University, 2015

Submitted to the Institute for Graduate Studies in  
Science and Engineering in partial fulfillment of  
the requirements for the degree of  
Master of Science

Graduate Program in Systems and Control Engineering  
Boğaziçi University

2018

## ACKNOWLEDGEMENTS

I would like to offer my sincere gratitude to my supervisor Prof. Dr. Yağmur Denizhan for her precious guidance, advice and support that she has shown. She has spent countless hours working with me throughout this research and has inspired and motivated me by her attitude towards problems.

I am also thankful to the members of thesis jury, Prof. Neslihan Serap Şengör and Assoc. Prof. Halil İ. Baştürk for participating in my thesis jury and for their valuable comments on the thesis.

My sincere thanks goes to Dr. Leyla Özkan for accepting me for the summer internship in Control Systems group and Dr. Bahadır M. Saltık who has led me working on his exciting project in an international environment and supported me along the way. It was great to have the opportunity to work in such a professional group in Eindhoven University of Technology.

I am also grateful to Viktor Novichenko from Vilnius University for his unrequited support and detailed answers to my questions.

I would like to thank all my friends who helped me get through this thesis for their continuous support and encouragement.

I owe a huge debt of gratitude to my family especially to my mother for her endless love and for being the most caring parent anybody could ask for, always being there for me despite all the obstacles. I should also thank to my father for always being supportive of my decisions in life. Finally, I must express my profound gratitude to Yankı for every moment we have spent and for always believing in me throughout my years of study and through this thesis.

*To my mother...*

## ABSTRACT

### **A DELAYED FEEDBACK BASED PRACTICAL CHAOS CONTROL METHOD: TAIL APERTURE FEEDBACK**

Control of chaotic systems has been one of the central issues in the field of chaotic dynamics since early 1990s. A particularly simple and practical method is the Delayed Feedback Control (DFC) introduced by Kestutis Pyragas, to stabilize chaotic systems at an Unstable Periodic Orbit (UPO). The basic idea of the DFC method is to apply an additive control input that is proportional to the difference between the current state and the state of the system delayed by the period of the target UPO. Since the DFC method only requires the knowledge of the period of the UPO, it has attracted great interest and has been applied to many systems. To render the method even more feasible and applicable various modifications and extensions of the original DFC have been presented in the literature.

In this thesis, a practical variant of the DFC, namely the Tail Aperture Feedback (TAF) method has been proposed that combines the basic approach of the DFC with some ideas borrowed from the OGY type chaos control. A practical procedure has been introduced for selecting the relevant parameters and applying the TAF method. Moreover, an original sparsification method has been presented which reduces the stored data. The performances of basic DFC method and the TAF method have been compared and the improvement provided by the sparsification method has been demonstrated on basis of simulation results.

## ÖZET

# GEÇİKMELİ GERİ BESLEMeye DAYALI PRATİK BİR KAOS KONTROLÜ YÖNTEMİ: KUYRUK AÇIKLIĞI GERİ BESLEMESİ

1990'ların başından bu yana, kaotik sistemlerin kontrolü kaotik dinamik alanının önemli konularından olmuştur. Kestutis Pyragas tarafından ileri sürülen gecikmeli geri besleme yöntemi (DFC) kaotik sistemleri bir kararsız periyodik yörünge üzerinde kararlı kılmak için kullanılan basit ve pratik bir yöntemdir. DFC yönteminin temel fikri sistemin mevcut durumu ile hedeflenen kararsız periyodik yörünge periyodu kadar önceki durumunun farkı ile orantılı bir kontrol girişi kullanılmasıdır. DFC yöntemi sadece kararsız periyodik yörünge periyodu bilgisini gerektirdiği için, büyük ilgi görmüş ve birçok sisteme uygulanmıştır. Yöntemi daha da elverişli ve uygulanabilir hale getirmek için orjinal DFC yönteminin çeşitli uyarlama ve uzantıları literatüre sunulmuştur.

Bu tezde, DFC yönteminin pratik bir varyantı olup DFC temel yaklaşımını OGY türü kaos kontrolden gelen bazı fikirlerle birleştiren kuyruk açıklığı geri besleme (TAF) yöntemi önerilmiştir. olarak adlandırılan başta olmak üzere çeşitli kaos kontrolü yöntemleri incelenmiştir. İlgili parametrelerin seçimi ve TAF yönteminin uygulanması için pratik bir prosedür önerilmiştir. Buna ek olarak, depolanan veriyi azaltmak için özgün bir seyreltme yöntemi sunulmuştur. Temel DFC ve TAF yöntemlerinin performansları karşılaştırılmış ve seyreltme metodu ile sağlanan gelişme simülasyon sonuçları üzerinden gösterilmiştir.



4.2.1. Stage 1: Filling the registers . . . . .	33
4.2.2. Stage 2: Updating the registers . . . . .	34
4.3. Performance Evaluation of TAF . . . . .	36
4.3.1. Comparison of the original DFC and the TAF method . . . . .	37
4.3.2. Comparison of the TAF method with and without Sparsification	38
5. DISCUSSION AND CONCLUSION . . . . .	40
REFERENCES . . . . .	41
APPENDIX A: DYNAMICAL SYSTEMS FUNDAMENTALS . . . . .	45
APPENDIX B: STABILITY DEFINITIONS . . . . .	48
B.1. Linearization and Local Stability . . . . .	48
B.2. Lyapunov Stability Related Definitions and Theorems . . . . .	49
APPENDIX C: FLOQUET STABILITY THEORY . . . . .	51

## LIST OF FIGURES

Figure 2.1.	One of the most investigated strange attractors: Lorenz Attractor.	7
Figure 2.2.	An illustration of the Poincaré surface of section in 3-D space and piercing points of the chaotic flow . . . . .	9
Figure 3.1.	The block diagram of the DFC method for the stabilization of a T-periodic UPO, where $y(t)$ is the measurable output signal and $u(t) = K[y(t - T) - y(t)]$ is the control input. . . . .	12
Figure 3.2.	Trajectory near a periodic orbit with (a) finite torsion ( $\Omega \neq 0$ ) and (b) no torsion ( $\Omega = 0$ ) . . . . .	14
Figure 3.3.	Three qualitatively different configurations of the Floquet multipliers of a UPO without control . . . . .	16
Figure 3.4.	Three qualitatively different configurations of the Floquet multipliers of a UPO with control . . . . .	16
Figure 4.1.	Illustration of the tail aperture vector at time $t$ for a hypothetical 3-D continuous-time system: $\Delta_T(t) = [\mathbf{x}(t) - \mathbf{x}(t - T)]$ , where the red line shows the system trajectory during the last $T$ units of time and the black line represents the earlier part of the trajectory. . .	21
Figure 4.2.	$\ \Delta_{5.89}(t)\ $ as a function of time for an uncontrolled Rössler system, here, the red line expresses the average of the local minima $\epsilon^* = 3.643$ , $t^* = 85.74$ , $\ \Delta_T(t^*)\  = 0.1146$ , and $\mathbf{x}^* = \mathbf{x}(t^* - T)$ . . . . .	26

Figure 4.3.	$\log_{10} \ \Delta_{\mathbf{T}}(t)\ _{rms}$ as a function of K in Rössler system for $T = 5.89$ , where $K_{cand}^* = 0.28$ . . . . .	27
Figure 4.4.	$\langle \ \dot{\mathbf{x}}\  \rangle_{test}$ as a function of K, here the blue line illustrates $\langle$ $\ \dot{\mathbf{x}}\  \rangle_{uncont} = 0.0927$ . . . . .	27
Figure 4.5.	Stabilized period-5.89 UPO of the Rössler system . . . . .	28
Figure 4.6.	$\ \Delta_{5.89}(t)\ $ as a function of time under the control of the TAF method with $K_{cand}^* = 0.28$ and $\epsilon^* = 3.643$ . . . . .	29
Figure 4.7.	The first component of the input vector as a function of time under the control of the TAF method with $K_{cand}^* = 0.28$ and $\epsilon^* = 3.643$ . . . . .	29
Figure 4.8.	$\ \Delta_{1.56}(t)\ $ as a function of time for an uncontrolled Lorenz system, here, the red line expresses the average of the local minima $\epsilon^* =$ $8.735$ , $t^* = 80.44$ , $\ \Delta_{\mathbf{T}}(t^*)\  = 0.3484$ , and $\mathbf{x}^* = \mathbf{x}(t^* - T)$ . . . . .	30
Figure 4.9.	$\log_{10} \ \Delta_{\mathbf{T}}(t)\ _{rms}$ as a function of K in Lorenz system for $T = 1.56$ where $K_{cand}^* = 0.6$ . . . . .	31
Figure 4.10.	$\langle \ \dot{\mathbf{x}}\  \rangle_{test}$ as a function of K, here the blue line illustrates $\langle$ $\ \dot{\mathbf{x}}\  \rangle_{uncont} = 1.077$ . . . . .	31
Figure 4.11.	Filling the time and state registers in the sparsification algorithm . . . . .	33

## LIST OF TABLES

Table 4.1.	Main aspects of the best known chaos control methods applicable to continuous time systems . . . . .	36
Table 4.2.	Comparison of the TAF and DFC methods applied to a chaotic Rössler system with $T = 17.5$ and $K = 0.2$ ( $\hat{t}_{st}$ calculated according to the same $\epsilon^*$ for both methods) . . . . .	37
Table 4.3.	Comparison of the TAF and DFC methods applied to a chaotic Rössler system with $T = 35.01$ and $K = 0.9$ ( $\hat{t}_{st}$ calculated according to the same $\epsilon^*$ for both methods) . . . . .	38
Table 4.4.	The dependence of the average size of stored data and of the quality of stabilization on the sparsification factor $k_{th}$ . . . . .	39

## LIST OF SYMBOLS

<b>A</b>	State matrix
<b>B</b>	Input matrix
<b>K</b>	Control matrix
$K_{\text{cand}}^*$	Control gain candidate
$k_{\text{th}}$	Sparsification factor
$n$	Dimension of a system
<b>P</b>	Poincaré map
$\mathbf{p}_{\text{nom}}$	Nominal values
$\hat{P}_{\text{rms}}$	Control power expenditure
$\mathbf{R}_K$	A reasonable range of control gains
$\mathbf{S}_P$	Poincaré surface of section
$T$	Period of the UPO
$T_{\text{run}}$	Period of the UPO
$\hat{t}_{\text{st}}$	Stabilization time
$\langle \ \dot{\mathbf{x}}\  \rangle_{\text{test}}$	Time average of the flow magnitude while applying TAF control
$\langle \ \dot{\mathbf{x}}\  \rangle_{\text{uncont}}$	Time average of the flow magnitude along the target UPO in an uncontrolled run
$\Delta_{\mathbf{T}}$	Tail aperture vector
$\epsilon$	Tail aperture tolerance
$\lambda$	Real part of the Lyapunov exponent
$\mu$	Floquet Multiplier
$\Omega$	Imaginary part of the Lyapunov exponent
$\tau_i$	Registered time instants
$\Phi$	State transition matrix
$\Psi$	Monodromy matrix
$\xi$	State of a discrete time system

**LIST OF ACRONYMS/ABBREVIATIONS**

2-D	Two Dimensional
3-D	Three Dimensional
DDE	Delayed Differential Equations
DFC	Delayed Feedback Control
EDFC	Extended Delayed Feedback Control
FE	Floquet Exponent
FM	Floquet Multiplier
OGY	Ott-Grebogi-Yorke
ONL	Odd Number Limitation
PBC	Prediction Based Feedback Control
PFC	Proportional Feedback Control
RMS	Root Mean Square
UDFC	Unstable Delayed Feedback Control
UEDFC	Unstable Extended Delayed Feedback Control
UPO	Unstable Periodic Orbit

## 1. INTRODUCTION

Over many years, chaos has been an interesting phenomenon in nature and has been shown to exist in many natural systems from meteorology to biology. With his research on the three-body problem, Henri Poincaré became the first person who laid the groundwork for modern chaos theory at the end of the 19<sup>th</sup> century. He pointed out that for some deterministic systems, small differences in the initial conditions may lead to enormous differences in the final phenomena. This is the first known published statement of the property now known as “sensitivity to initial conditions”, which is one of the defining properties of a deterministic chaotic dynamical system. Later, in the second half of the 20<sup>th</sup> century, Edward Lorenz, an American meteorologist, while simulating partial differential equations that describe the turbulent motion of the atmosphere, discovered that under certain conditions deterministic systems can behave in an unpredictable manner. Deterministic chaos has become a widely investigated topic since Edward Lorenz published his paper “Deterministic Nonperiodic Flow” in the Journal of the Atmospheric Sciences in 1963 [1]. After the first usage of the word ‘chaos’ in the scientific literature by Li and Yorke in 1975 [2], increasing number of articles has been published on this subject, and chaos has become a significant topic in mathematics. In 1883, German mathematician Georg Cantor published a paper in which describes what would come to be known as the “Cantor set” [3] later called fractals by Mandelbrot. As computers became a powerful tool at the end of the 1970’s, Mandelbrot discovered a structure with self-similarity at all scales while visualizing a noisy data and introduced fractal geometry [4]. Fractals gained significance because chaotic systems have attractors that mostly exhibit fractal properties and helped characterizing the complicated structures of *strange attractors* (also known as chaotic attractors). Typically, there exist infinitely many Unstable Periodic Orbits (UPOs) embedded in the strange attractor and generally one of them is chosen to be stabilized in chaos control methods.

Chaos theory was not developed by a single person or a single team of scientists, but rather it was the product of different scientists working on different problems.

According to Strogatz [5], deterministic chaos can be defined as the aperiodic long-term behavior in a deterministic system that shows sensitive dependence on I.C.s. While there exists a variety of rather simple differential and difference equations exhibiting chaotic behavior in the literature, such as the Logistic equation, the Henon map, the Rössler system and Chua's circuit, chaos is also observable in real systems; e.g. in population dynamics, psychology, biology, medicine, chemical reactions, mechanical movements etc..

At the beginning of 1990s some researchers came up with the idea of controlling chaotic systems. Usually, closed-loop control of a dynamic system means that the system is made to converge to and stay on an arbitrary, externally specified target behavior by applying feedback-based inputs. However, in almost all versions of chaos control the target behavior is chosen as one of the infinitely many unstable periodic orbits embedded in strange attractor, such that the control task reduces to the feedback-based stabilization of an inherent (yet unstable) behavior of the system.

Following the first chaos control method proposed by Ott, Grebogi and Yorke (OGY) [6] many alternative methods have been suggested by various researchers. However, all of them share the common feature that the target behavior is an unstable periodic orbit (or in some cases an equilibrium point, which can be considered as a periodic orbit with period zero) embedded in the strange attractor. The OGY method is based on the following idea: A chaotic system's behavior on its strange attractor - by its very nature -, guarantees that a close neighborhood of any point on it will be visited within finite time. When the system trajectory enters a close neighborhood of the target UPO, the control parameters of the system are varied appropriately with a limited range to stabilize the target. Over the years, to improve the performance of the method, some modified OGY methods have been proposed [7–10].

In 1992, Pyragas proposed a method [11] that addresses a slightly different control task: Here, the aim is to stabilize the chaotic system at one of its UPOs with a specified period. The method requires the knowledge that at least one UPO with that period exists but nothing about its whereabouts. The method uses delayed feedback to make

the system converge to and stay on a UPO with the specified period, however, there may be more than one such UPOs. In this case, it will depend on the initial conditions to which one the system will converge. The delayed feedback control (DFC) algorithm uses a control input, which is proportional to the difference between the current output of the system and the output of the system delayed by period of the target orbit.

As the only information required about the target orbit is its period, this new method has attracted great interest among experimentalists, giving rise to applications in different fields such as chemistry, biology, medicine, economy and engineering. As the method was employed extensively, some limitations were identified from the analysis of the initially proposed DFC and many modifications were proposed to improve its performance (see the surveys [12–15]).

One of the problems of the DFC algorithm is that it fails to control orbits with long periods. To overcome this problem, the most popular modification of the original DFC scheme is the so-called Extended Delayed Feedback Control (EDFC) has been introduced [16]. The EDFC scheme uses information from many previous states of the system to stabilize orbits with larger periods, which are not stabilizable by the original DFC [17].

As delayed feedback leads to delayed differential equations, it is quite difficult to analyze the stability and to propose an analytical stabilization criterion for the control gain. In 2012, Pyragas noted that “Even linear analysis of such systems is complicated due to the infinite number of Floquet exponents characterizing the stability of controlled orbits.” [14]. Nevertheless, some general analytical results and properties have been obtained about the algorithm throughout the years [18–21].

In 1997, Nakajima [19] proved the existence of the so-called *Odd Number Limitation* (ONL); that is, unstable periodic orbits with an odd number of real Floquet multipliers (FMs) larger than unity cannot be stabilized by time-delayed feedback control (DFC). Nonetheless, in 2007, Fiedler *et al.* [22] showed by a simple example that this limitation does not hold in general for autonomous systems (note that for non-

autonomous systems it remains valid in general). Recently, a modified proof (“corrected ONL”) of the limitation for autonomous systems has been presented by Hooton and Amann [23]. To bypass this limitation in autonomous systems, some control matrix design algorithms have been proposed for DFC by using Hooton and Amann’s criterion [24].

In this thesis, delayed feedback type control of continuous-time chaotic systems has been investigated and a practical method, the Tail Aperture Feedback (TAF), has been developed, which combines the basic approach of DFC with some ideas borrowed from OGY type chaos control with the basic concern of keeping the a priori knowledge about the system dynamics at a minimum level.

The thesis is organized as follows: In Section II, basic theoretical definitions of chaotic dynamics and chaos control are provided. In Section III, DFC method used in control of chaotic systems is explained in detail where the theory behind the method as well as the extensions and limitations of the method are provided. Proposition and investigation of the TAF method that is used to control chaotic systems are given in Section IV. Theoretical basis and the procedure of the TAF method are explained for continuous-time systems. Moreover, a practical sparsification algorithm is provided to reduce the stored data and its performance is shown on the TAF method. Finally, in Section V, discussion and concluding remarks on the TAF method, sparsification algorithm and future works are provided.

## 2. THEORETICAL FOUNDATION

### 2.1. Chaotic Dynamics

Dynamical systems can be represented in terms of mathematical models which describe the laws that govern how the system changes. Depending on the nature of the system at hand, as well as the availability of information about it, one may have to employ *stochastic models*, which express the rules that govern probabilities of changes in the system, or *deterministic models*, which describe how the change in the system states are related to the present and past states, and possibly to external inputs. We can subdivide the systems, the behaviors of which can be expressed as deterministic laws in terms of a finite number of system states, into two main categories: systems that change continuously in time and those that can change only at discrete time instances. The former are typically described via differential equations, and the latter via difference equations. *Continuous time systems* can be represented in the following general form:

$$\dot{\mathbf{x}}(t) = \mathbf{f}(\mathbf{x}(t), \mathbf{u}(t), t) \quad (2.1)$$

Similarly, *discrete time systems* can be represented as follows,

$$\mathbf{x}(k+1) = \mathbf{f}(\mathbf{x}(k), \mathbf{u}(k), k) \quad (2.2)$$

where  $\mathbf{x}(t), \mathbf{x}(k) \in \mathbf{R}^n$  represent state vectors and  $\mathbf{u}(t), \mathbf{u}(k) \in \mathbf{R}^m$  represent the input vectors, respectively and  $\mathbf{f}$  is an  $n$ -dimensional vector function called the *system function*.

Among such deterministic dynamic systems particularly the dissipative ones, i.e. those that settle down to an “attracting” steady state behavior, are of practical importance. Such “attracting behaviors” can be subdivided into: (i) *point attractors* (attracting equilibrium points), (ii) *periodic attractors* (attracting periodic orbits) and

(iii) *strange (chaotic) attractors.*

The deterministic systems considered in this thesis are those that have strange attractors and are characterized by long term aperiodic behavior and sensitive dependence on initial conditions. The *sensitivity to initial conditions* means that nearby system trajectories diverge from each other exponentially fast (on average). Continuous-time systems that combine this kind of exponential divergence of nearby trajectories and dissipativeness can exist only from 3-D onward.

*Lyapunov exponents* constitute a measure for the convergence or divergence of nearby trajectories. An  $n$ -dimensional system has  $n$  Lyapunov exponents, which express the exponential rate of convergence or divergence of nearby trajectories in the associated  $n$  eigen-directions of the flow. Positive Lyapunov exponents indicate divergence, while, negative ones indicate convergence. For dissipative systems the sum of the Lyapunov exponents has to be negative [25], implying that under the governing dynamics phase space (hyper-)volumes shrink down to an attractor of measure zero. On the other hand, sensitivity to initial conditions, which is a characteristic feature of dissipative chaos, entails at least one positive Lyapunov exponent. As a result, the strange attractor of any dissipative chaotic system is a fractal structure that has zero phase (hyper-)volume, and occupies a finite region of the phase space. (Figure 2.1 shows strange attractor of the Lorenz system.)

Typically, there exist infinitely many *Unstable Periodic Orbits* (UPOs) embedded in the strange attractor of a dissipative chaotic system. These UPOs have saddle type of instability, meaning that the periodic orbit exhibits an attracting behavior in some directions, while exhibiting repelling behavior in some other directions. Most of the studies on chaotic systems are related to the steady state behavior on the strange attractor, while the transient behavior until the system reaches the attractor is usually discarded.

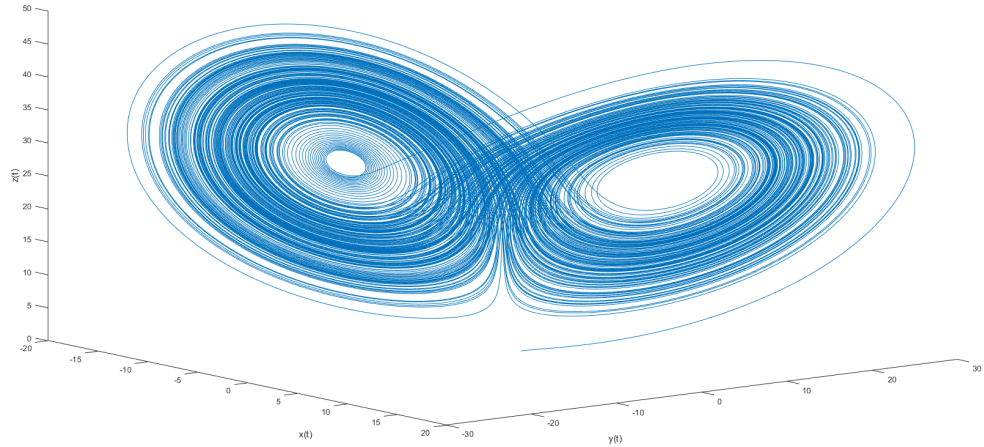


Figure 2.1. One of the most investigated strange attractors: Lorenz Attractor.

## 2.2. Chaos Control

In spite of their seemingly irregular character, deterministic chaotic systems can be controlled by applying some appropriate feedback. However, chaos control as known in the literature has a slightly different goal statement than the control of dynamic systems in general, which refers to the act of forcing the system to behave in an externally specified manner, i.e. to follow an externally given reference trajectory. In almost all versions of chaos control the reference is one of the infinitely many UPOs embedded in the strange attractor (from here onward it will be mentioned as *the target UPO*). Hence, controlling chaos is a very specific type of closed-loop control, where the reference trajectory is chosen from the inherent repertoire (the set of UPOs) of the chaotic system.

Following the first chaos control method proposed in 1990 by Ott, Grebogi and Yorke (OGY) [6], many alternatives have been suggested by various researchers. The OGY control method is based on the following idea: the very nature of a chaotic system's behavior on its strange attractor guarantees that starting from an arbitrary

initial condition, any finite region of the strange attractor will be reached within finite time. Hence, OGY control remains inactive until the system enters by itself a close enough neighborhood of the target UPO, and is only activated when the system is within that neighborhood, the *OGY region* ( $\Omega_{OGY}$ ). The control task, which can be defined as the stabilization of the target UPO, is achieved by slightly varying some of the parameters (the control parameters,  $\mathbf{p}$ ) of the system. In the OGY control method, the continuous time control problem is converted into a discrete one by introducing a Poincaré surface  $\mathbf{S}_p$  (an (n-1)-dimensional hypersurface in the n-dimensional state space) and considering the time instances, when the system trajectory traverses the surface in a specified direction (Figure 2.2). Denoting the  $k^{th}$  piercing point by  $\boldsymbol{\xi}(k)$ , the so-called Poincaré map  $\mathbf{P}$  can be found, which associates successive piercing points as in (2.3). Here,  $\mathbf{p}$  denotes the vector of control parameters.

$$\boldsymbol{\xi}(k+1) = \mathbf{P}(\boldsymbol{\xi}(k), \mathbf{p}) \quad (2.3)$$

If there exists a UPO traversing the  $\mathbf{S}_p$ , then it has to do so piercing the surface at  $\boldsymbol{\xi}^*$ , which is a period-1 point (i.e. an equilibrium point as seen in Figure 2.2) or a higher periodic point of the Poincaré map  $\mathbf{P}$ . Here, for the sake of simplicity, the method will be presented only for a UPO that traverses the Poincaré surface at an equilibrium point  $\boldsymbol{\xi}^*$ . As a preparation for the OGY control, data are gathered from the system while varying the control parameters randomly within a narrow range ( $U_{OGY}$ ) about their nominal values ( $\mathbf{p}_{nom}$ ), and a local linear estimate for (2.4) is obtained as follows:

$$\boldsymbol{\xi}(k+1) = \mathbf{P}(\boldsymbol{\xi}(k), \mathbf{p}) \approx \mathbf{A}\boldsymbol{\xi}(k) + \mathbf{B}(\mathbf{p}(k) - \mathbf{p}_{nom}) = \mathbf{A}\boldsymbol{\xi}(k) + \mathbf{B}\mathbf{u}(k) \quad \forall \boldsymbol{\xi}(k) \in \Omega_{OGY} \quad (2.4)$$

where  $\mathbf{A} = \left. \frac{\partial \mathbf{P}(\boldsymbol{\xi}, \mathbf{p})}{\partial \boldsymbol{\xi}} \right|_{\boldsymbol{\xi}=\boldsymbol{\xi}^*, \mathbf{p}=\mathbf{p}_{nom}}$  and  $\mathbf{B} = \left. \frac{\partial \mathbf{P}(\boldsymbol{\xi}, \mathbf{p})}{\partial \mathbf{p}} \right|_{\boldsymbol{\xi}=\boldsymbol{\xi}^*, \mathbf{p}=\mathbf{p}_{nom}}$ .

The equilibrium point  $\boldsymbol{\xi}^*$  of the Poincaré map for  $\mathbf{p} = \mathbf{p}_{nom}$  is given by

$$\boldsymbol{\xi}^* = \mathbf{P}(\boldsymbol{\xi}^*, \mathbf{p}_{nom}) \quad (2.5)$$

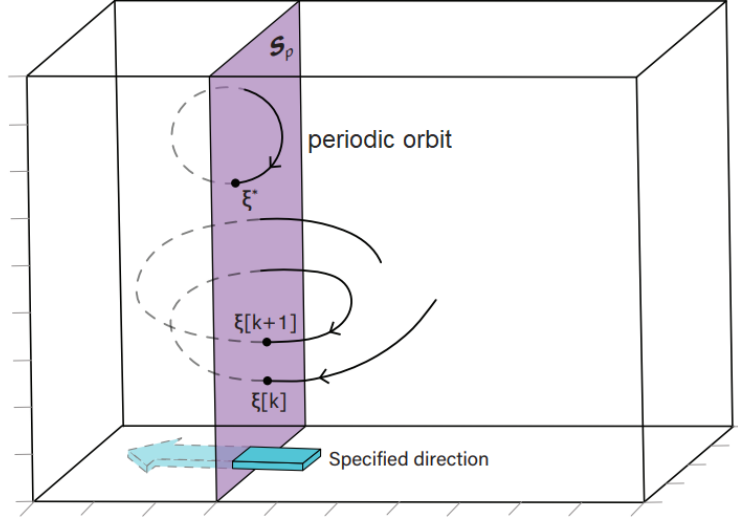


Figure 2.2. An illustration of the Poincaré surface of section in 3-D space and piercing points of the chaotic flow

The control law can be formulated as

$$\mathbf{u}_{OGY}(k) = \mathbf{p}(k) - \mathbf{p}_{nom} = \begin{cases} \mathbf{K}(\boldsymbol{\xi}(k) - \boldsymbol{\xi}^*), & \text{if } \boldsymbol{\xi}(k) \in \Omega_{OGY}. \\ 0, & \text{otherwise.} \end{cases} \quad (2.6)$$

where  $\mathbf{K}$  can be designed (relying on the local linear model (2.4) by any linear control method (e.g. pole placement) to make  $\boldsymbol{\xi}^*$  stable. The stability of the Poincaré map exhibits the same stability properties as the associated UPO of the original system.

In 1992, Pyragas proposed two new methods for the stabilization of the periodic orbits: the *Delayed Feedback Control* (DFC) and the *Proportional Feedback Control* (PFC) [11]. While the DFC method uses one of the output signals delayed by the period of the target UPO as reference (3.3), the PFC method uses the complete description of the target UPO as a reference. The closed-loop dynamics obtained by the PFC method can be expressed as follows,

$$\dot{\mathbf{x}}(t) = \mathbf{f}(\mathbf{x}(t)) + \mathbf{G}(\mathbf{x}^* - \mathbf{x}(t)) \quad (2.7)$$

where  $\mathbf{G}$  is the control gain matrix, which is found from the *monodromy matrix*  $\Psi(t)$  (the state transition matrix over a period  $[t, t+T]$ ,  $\Phi(t+T, t)$ ). Monodromy matrix can be calculated by integrating the variational equations (2.8) of the closed-loop system around the target UPO for one period ( $T$ ) as follows

$$\frac{d\Phi(t, 0)}{dt} = [\nabla_x \mathbf{f}(t, \mathbf{x}, \mathbf{u}) - \nabla_u \mathbf{f}(t, \mathbf{x}, \mathbf{u})\mathbf{G}]|_{\mathbf{x}=\mathbf{x}^*(t)} \Phi(t, 0), \quad t \in [0, T], \quad \Phi(0, 0) = \mathbf{I}_n \quad (2.8)$$

According to the Floquet theory (Appendix C),  $\mathbf{G}$  is chosen such that the largest Floquet Multiplier of the monodromy matrix is minimized. The need for a priori knowledge about the entire UPO is the principal disadvantage of the PFC method.

Another chaos control method proposed for the stabilization of a target UPO is the *Prediction-Based Feedback Control* (PBC). In 1999, Ushio and Yamamoto introduced a state feedback control method, which uses the predicted values of the states [26]. In contrast to control that is based on the past states as in the DFC case, the control in PBC method uses the predicted states one period ahead, computed along the trajectories of the free system response. The closed-loop dynamics obtained by the PBC method can be expressed as

$$\dot{\mathbf{x}}(t) = \mathbf{f}(\mathbf{x}(t)) + \mathbf{M}(\phi(t+T, t, \mathbf{x}(t), 0) - \mathbf{x}(t)) \quad (2.9)$$

where  $\phi(t+T, t, \mathbf{x}(t), 0)$  is the value at time  $(t+T)$  of the state starting from  $\mathbf{x}(t)$  at time  $t$  of the uncontrolled system and  $\mathbf{M}$  is the control gain matrix. The main disadvantage of the PBC method is the need for a priori knowledge of the system equations, which may not always be satisfied.

### 3. CHAOS CONTROL VIA DFC

In 1992, Pyragas proposed a simple and convenient method of controlling chaos, the so-called Delayed Feedback Control (DFC) [11]. As mentioned earlier, DFC is based on a control proportional to the difference between the measurable current output signal and a delayed output signal. The delay time is taken as the period of the target UPO such that the control input vanishes when the system is on the UPO. The most important advantage of the DFC method is that it does not require any a priori information about the UPO except for its period. As the DFC method does not require any real-time processing or any a priori knowledge about the target UPO (except for its period  $T$ ) this new method has attracted great interest among experimentalists from various fields such as chemistry, biology, medicine, economy and engineering, leading to applications on real systems such as an atomic force microscope [27], a high-speed semiconductor laser system [28] or a magnetoelastic system [29]. As the method was employed extensively, some limitations of the initially proposed DFC have been discovered and many modifications have been proposed to improve its performance (see the surveys [12–15]). Let us consider an uncontrolled dynamic system

$$\dot{\mathbf{x}}(t) = \mathbf{f}(\mathbf{x}(t), 0) \quad (3.1)$$

with the system states  $\mathbf{x}(t) \in \mathbb{R}^n$ , the control input  $u(t) = 0$  and  $\mathbf{f} : \mathbb{R}^n \rightarrow \mathbb{R}^n$ . Suppose that the system has a  $T$ -periodic UPO denoted as  $\mathbf{x}^*(t) = \mathbf{x}^*(t - T)$ . The original DFC method uses a scalar control input which corresponds to the measurable output state of the system. The following form is used for the DFC method:

$$\dot{\mathbf{x}}(t) = \mathbf{f}(\mathbf{x}(t), u(t)) \quad (3.2)$$

$$u(t) = K[y(t - T) - y(t)] \quad (3.3)$$

where  $y(t) = \mathbf{g}(\mathbf{x}(t))$  is the scalar output variable. Delayed output signal  $y(t - T)$  is used as reference signal as seen in the block diagram of the DFC method in Figure 3.1

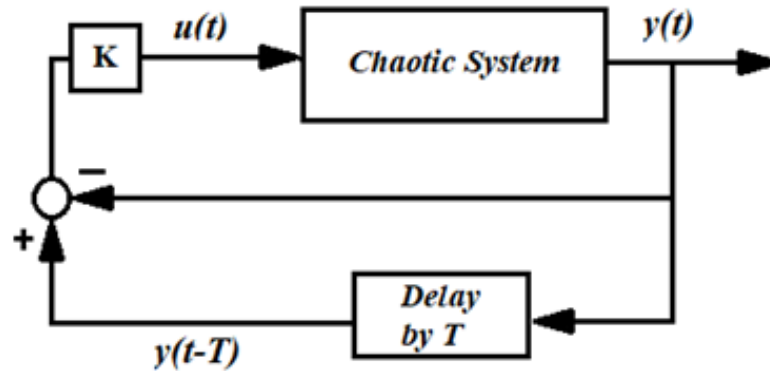


Figure 3.1. The block diagram of the DFC method for the stabilization of a  $T$ -periodic UPO, where  $y(t)$  is the measurable output signal and  $u(t) = K[y(t - T) - y(t)]$  is the control input.

As the DFC method involves nonlinear Delay Differential Equations (DDE), it is quite difficult to analyze its stability and give some analytical stabilization criteria. Even local linear analysis of such systems is highly complex due to the fact that an infinite number of Floquet exponents result from the delay term. Nevertheless, some general analytical results about the DFC have been presented in the literature [18–21].

### 3.1. Design of the Control Gain Matrix

In the paper published in 1992 [10], Pyragas proposed a constant scalar control gain  $K$  for the DFC method. However, since the closed-loop system includes Delayed Differential Equations (DDEs), it is quite difficult to analyze its stability and give analytical stabilization criteria for the control gain. Therefore, the control gain that stabilizes the target UPO found empirically. Application of the DFC with constant gain in practical experiments and theoretical models can be found in [14].

In general, a scalar gain  $K$  is chosen by using the information of the largest Lyapunov exponent, which, on periodic orbits, corresponds to the real part of the Floquet exponent (or also called characteristic exponents). In [11], the control gain  $K$  is chosen such that the largest Lyapunov exponent of the periodic orbit becomes negative. As explained in [30, 31], the largest Lyapunov exponent can be estimated from the output time series of a dynamical system or calculated (numerically) using its mathematical model. However, such estimation and calculations require not only much computational effort but also the complete description of the target UPO, which is typically not available.

Another empirical approach for selecting the control gain  $K$  is to calculate the average distance between the current state and the delayed state for different  $K$  values and to select a  $K$  value which provides the lowest average distance, as explained in [11]. Since this approach does not require the complete description of the target UPO, it is more practical than using the largest Lyapunov exponent to choose a suitable control gain.

Later in 1995, Pyragas developed another approach to decide a stabilizing control matrix for the DFC [17]. According to that, the main stability properties of the system controlled by the DFC can be derived from a leading Floquet exponent defining the system behavior under the Proportional Feedback Control (PFC).

### 3.2. Extended Delayed Feedback Control

In 1994, Socolar, Sukow and Gauthier have introduced the best known extended version of the DFC, *Extended Delayed Feedback Control* (EDFC). EDFC uses not only one delayed state  $y(t - T)$  as in (3.3), but the sum of the, ideally infinite, terms  $y(t - mT)$ ,  $m = 1, 2, \dots, +\infty$  as shown in the following control rule [16].

$$u(t, y(t)) = K[(1 - R) \sum_{m=1}^{\infty} R^{m-1} y(t - mT) - y(t)] \quad (3.4)$$

where  $0 \leq R < 1$  and  $K$  are experimentally adjustable constants and  $y(t)$  is the scalar output variable. Constant  $R$  value can be considered as a memory parameter which weights information of the past states. For  $R = 0$ , (3.4) turns into the control law in the original DFC algorithm [15]. Although EDFC introduces an improvement in DFC concerning the stabilization of UPOs with larger periods that are not stabilizable by the original DFC, the form of EDFC is not very suitable for real applications because it requires storing information of all states in the past.

### 3.3. Odd Number Limitation

A short time after the proposal of DFC, it has been noticed that certain UPOs cannot be stabilized by the original DFC method. The underlying reason has been found to be related to a phenomenon called the odd number limitation (ONL), which refers to the fact that any UPO with an odd number of real Floquet multipliers (FMs) greater than unity can never be stabilized by the DFC method. This limitation was first proven by Ushio for discrete-time systems [18]. Just *et al.* showed that the DFC can stabilize only a certain class of periodic orbits characterized by a “finite torsion” [20]. More precisely, a periodic orbit with “finite torsion” means that the imaginary part of the Floquet exponent (FE) of the periodic orbit is non-zero. Physically, the real and imaginary parts of the Floquet exponent determines the departure from and the revolution around the desired periodic orbit, respectively as can be seen from Figure 3.2 below.

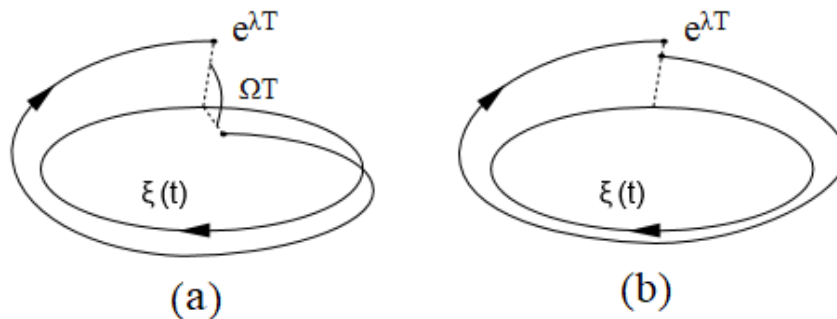


Figure 3.2. Trajectory near a periodic orbit with (a) finite torsion ( $\Omega \neq 0$ ) and (b) no torsion ( $\Omega = 0$ )

Stabilization of the periodic orbit is achieved if the positive real part of the Floquet exponent ( $\lambda$ ) becomes negative or the corresponding Floquet Multiplier ( $\mu$ ) becomes less than one in modulus. As stated in [20], control can be achieved by DFC only if there is a finite torsion ( $\Omega \neq 0$ ) when  $\lambda = 0$ . This necessity can also be understood from the observation of a trajectory near the desired periodic orbit in Figure 3.2. Difference between the points on such a trajectory become infinitesimally close after one period in the absence of torsion as in Figure 3.2(b). Since the control force is just proportional to the distance between these points, it vanishes before the desired orbit is reached and stabilization cannot be achieved. Thus, Just *et al.* explained the ONL as the necessity of finite torsion for stabilization via DFC, which yields constraints on the Floquet multipliers of the uncontrolled system.

In 1997, Nakajima proved the same limitation for the non-autonomous continuous-time systems and claimed in a footnote that the same proof can be extended to autonomous systems [19]. However, this extension to autonomous systems was later shown to be incorrect by B. Fiedler *et al.*, who provided a simple autonomous case example of stabilization of the UPO with one real positive unstable FM by DFC [22]. This paper has demonstrated that the ONL does not hold in general for autonomous systems (note that it remains valid for non-autonomous systems). To overcome the ONL several modified versions of the original DFC have been intensively discussed in the literature. One of best known methods used half-period delays for special symmetric orbits [32]. The other well-known method used the introduction of an additional, unstable degree of freedom [33] which are simply explained in Section 3.3.1 and Section 3.3.2, respectively. Recently, in 2012, a modified version of the limitation (corrected ONL) for continuous autonomous systems has been proven by Hooton and Amann [23]. It has also been shown that, by using the Hooton and Amann's criteria, the scenario presented by Fiedler can be achieved for new examples of autonomous systems [24].

For the sake of clarity, the ONL phenomenon can also be explained in terms of corresponding FMs ( $\mu$ ) on the Root Locus Diagram in discrete time. Since, a real FM cannot become complex without collision with another real FM, there can be only pairs of complex conjugate FMs. Thus, in case of an odd number of real FMs that are

greater than unity, at least one of them will be purely real, implying zero torsion.

Figure 3.3 and Figure 3.4 show a unit circle with FMs in the complex plane for an autonomous system. If all FMs are within the unit circle (except for the trivial FM, which equals to 1 and is shown in blue color), then the periodic orbit is stable. Figure 3.3 shows three conditions of the UPO in the absence of control (equivalent to DFC with  $K = 0$ ) and Figure 3.4 shows the same conditions under DFC with  $K > 0$ . The uncontrolled periodic orbit has an infinite number of FMs at the origin (green color) additional to the regular FMs. As the control gain increases, all FMs (except the trivial one at 1) start to move continuously as can be seen in Figure 3.4<sup>1</sup>.

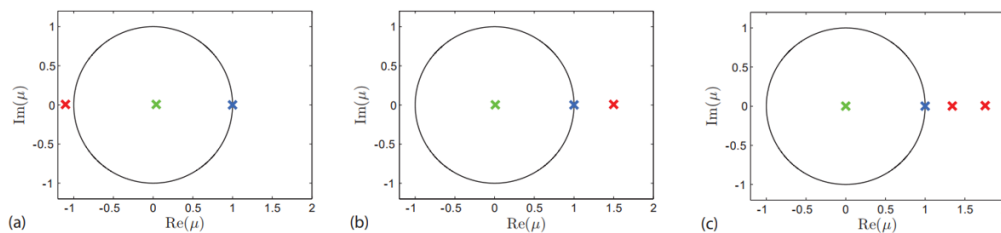


Figure 3.3. Three qualitatively different configurations of the Floquet multipliers of a UPO without control

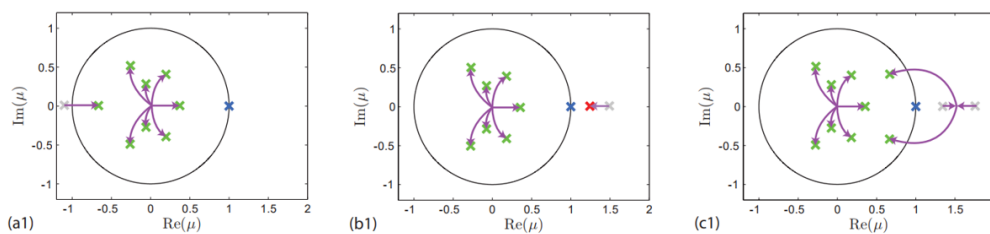


Figure 3.4. Three qualitatively different configurations of the Floquet multipliers of a UPO with control

For the condition in Figure 3.4(a1), the real negative unstable FM can enter the unit circle through the left side, since in principle all FMs can enter the unit circle through the left side regardless of how many there are. The situation for real positive

<sup>1</sup>Figure 3.3 and Figure 3.4 are taken from the personal conversation with Viktor Novicenko.

unstable FM/FMs is slightly different due to the trivial FM, which always stands at the right side of the unit circle in autonomous systems. If there are two (or an even number of) real positive unstable FMs as in Figure 3.4(c1), the possible stabilization scenario occurs when real FMs collide, become complex conjugate, and enter the unit circle from the right (above and below). As illustrated in Figure 3.4(b1), such a scenario is not possible for odd positive unstable FMs.

In [22] B. Fiedler *et al.* demonstrated an example of stabilization of the periodic orbit with a single real positive unstable FM by the DFC method. The stabilization scenario was exactly as in (b1), where the only real unstable FM enters the unit circle through the trivial FM. After that, in 2012, E. W. Hooton and A. Amann published a paper where the odd number limitation theorem was corrected and proven for autonomous systems (the so-called Hooton-Amann criterion) [23]. The corrected version of the ONL states that if there are an odd number of positive unstable FMs, the only possible stabilization scenario is when one FM goes through the trivial FM. So, to summarize, one can say that for autonomous systems the periodic orbit with an odd number of positive unstable Floquet multipliers can be stabilized via DFC provided that it satisfies the Hooton and Amann criterion.

### 3.3.1. Half-Period Delayed Feedback Control

In 1998, Nakajima and Ueda proposed a method called Half-Period Delayed Feedback Control to overcome the ONL [32]. However, this method is restricted to a special case of symmetric UPOs: the self-symmetric UPOs. Let us consider a nonautonomous system described by (3.5).

$$\dot{\mathbf{x}}(t) = \mathbf{f}(\mathbf{x}(t), t) \quad (3.5)$$

The system equation with the proposed Half-period DFC is defined as:

$$\dot{\mathbf{x}}(t) = \mathbf{f}(\mathbf{x}(t), t) - \mathbf{K}[\mathbf{x}(t - T/2) + \mathbf{x}(t)] \quad (3.6)$$

where  $\mathbf{K}$  is the control gain matrix and  $T/2$  is the half of the period of the target UPO. Thus, the additive control input does not necessarily vanish when a  $T$ -periodic UPO is stabilized, but it vanishes only when a self-symmetric orbit is stabilized. Hence, this method is capable of stabilizing self-symmetric UPOs.

### 3.3.2. Unstable Extended Delayed Feedback Control Method

Another method that aims to overcome the ONL is the *Unstable Delayed Feedback Control* (UDFC), which has been proposed by Pyragas in 2001 [33]. Here, the main idea is to increase the number of real Floquet multipliers greater than unity to an even number by introducing an unstable degree of freedom in the feedback loop. Later, in 2003, Pyragas extended the DFC method by combining this idea with the EDFC and developed the *Unstable Extended Delayed Feedback Control Method* (UEDFC). Hence, UEDFC method uses data from many previous states and eliminates the ONL by introducing an unstable degree of freedom into the feedback loop.

The system equation with the delayed feedback term is defined as:

$$\dot{\mathbf{x}}(t) = \mathbf{f}(\mathbf{x}(t), u(t)) \quad (3.7)$$

where the control input  $u(t) = KF_u(t)$  and  $K$  is a scalar control gain. Let  $y(t)$  denote a measurable scalar variable  $y(t) = g(\mathbf{x}(t))$ . The control input  $u(t)$  is determined by the following control law:

$$F_u(t) = F(t) + w(t), \quad (3.8)$$

$$\dot{w}(t) = \lambda_c^0 w(t) + (\lambda_c^0 - \lambda_c^\infty) F(t), \quad (3.9)$$

$$F(t) = y(t) - (1 - R) \sum_{k=1}^{\infty} R^{k-1} y(t - kT), \quad (3.10)$$

where  $F(t)$  is the form used in EDFC with  $0 \leq R < 1$  and  $w(t)$  is the unstable degree of freedom introduced into the feedback loop with  $\lambda_c^0 > 0$  and  $\lambda_c^\infty < 0$ . Whenever the stabilization of the target UPO is achieved,  $F(t)$  and  $w(t)$  and consequently the

feedback force  $F_u(t)$  vanish.

## 4. CHAOS CONTROL VIA TAF

In the previous chapters, the basic continuous-time chaos control methods known in the literature have been presented. In this thesis, an alternative practical method, dubbed the *Tail Aperture Feedback* (TAF) control, has been developed, which combines the basic approach of the DFC with some ideas borrowed from OGY-type chaos control, bearing in mind the basic concern of keeping a priori knowledge about the system dynamics at a minimum level. As will be explained below, the TAF approach basically requires only the prior knowledge of the period ( $T$ ) of the target UPO and the ability to store the state trajectory during the last  $T$  units of time.

### 4.1. TAF Method for Continuous-Time System

#### 4.1.1. Theoretical Basis

Let us consider a continuous-time dynamic system representable as in 4.1, where  $\mathbf{x}(t)$  and  $\mathbf{u}(t)$  correspond to the  $n$ -dimensional state vector and the  $n$ -dimensional additive control input vector, respectively.

$$\dot{\mathbf{x}}(t) = \mathbf{f}(\mathbf{x}(t)) + \mathbf{u}(t) \quad (4.1)$$

The TAF method uses a control law, which prescribes a control input that is proportional to  $\Delta_T(t) = [\mathbf{x}(t) - \mathbf{x}(t - T)]$ , which from here onward will be referred to as the “*tail aperture vector*” (Figure 4.1).

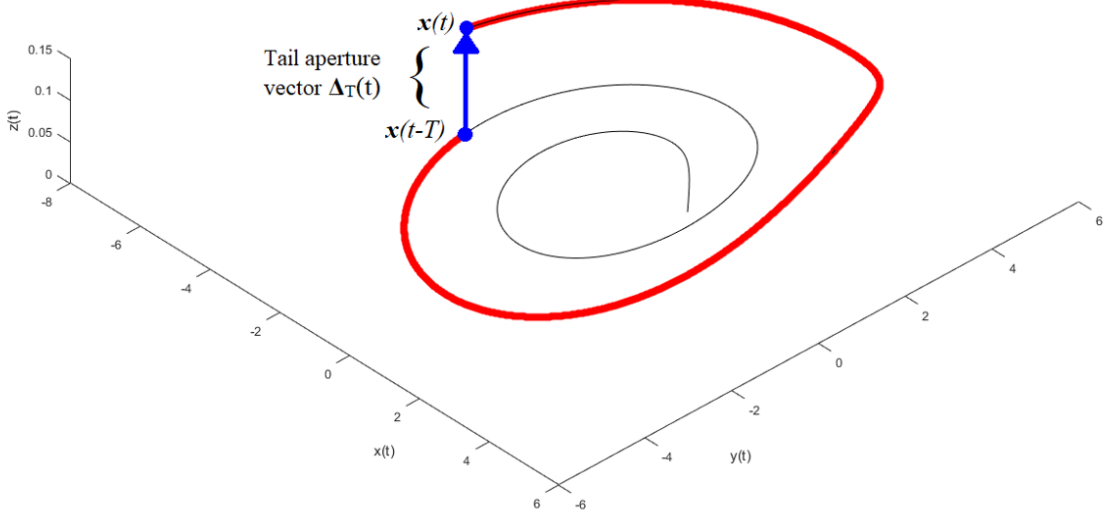


Figure 4.1. Illustration of the tail aperture vector at time  $t$  for a hypothetical 3-D continuous-time system:  $\Delta_T(t) = [\mathbf{x}(t) - \mathbf{x}(t - T)]$ , where the red line shows the system trajectory during the last  $T$  units of time and the black line represents the earlier part of the trajectory.

If the system is exactly on a  $T$ -periodic orbit, the tail aperture vector becomes zero while  $\|\Delta_T(t)\| \neq 0$  is an indicator of a deviation from a  $T$ -periodic behavior. This proportional control is applied as long as the tail aperture is reasonably small.

$$\mathbf{u}_{\text{TAF}}(t) = \begin{cases} -K\Delta_T(t), & \text{for } \|\Delta_T(t)\| < \epsilon^*. \\ 0, & \text{otherwise.} \end{cases} \quad (4.2)$$

where  $T$  is the period of the target UPO,  $K$  is the scalar control gain,  $\Delta_T(t) = [\mathbf{x}(t) - \mathbf{x}(t - T)]$  is the tail aperture vector, and  $\epsilon$  is the tail aperture tolerance. It should be noted that  $\mathbf{u}_{\text{TAF}}(t)$  can step in only  $T$  units of time after the start of the system because until then there is no data available to check the periodicity of the system trajectory. As can be seen, the TAF method can be considered as a special and modified version

of the DFC law,

$$u_{\text{DFC}}(t) = K[y(t - T) - y(t)] \quad (4.3)$$

where  $y(t)$  is a scalar output variable of the system and  $u_{\text{DFC}}(t)$  is the scalar control input. Hence, the difference between DFC and TAF is twofold:

(i) DFC uses delayed feedback based on a scalar output variable alone, while TAF uses full state feedback.

(ii) While DFC is applied everywhere in the state space, TAF is applied only when the system exhibits a nearly  $T$ -periodic behavior, and leaves the system uncontrolled otherwise in order to avoid too much alteration of the chaotic system characteristics.

In that respect, the TAF control resembles the basic OGY control, where control is applied in close vicinity of the target UPO, while relying on the fact that the trajectories -due to the uncontrolled dynamics of the chaotic system on its strange attractor- will eventually visit a narrow enough neighborhood of the target UPO within a finite time.

#### 4.1.2. Procedure

To apply the TAF method, two parameters need to be appropriately chosen: the scalar control gain  $K$  and the tail aperture tolerance  $\epsilon$ . Below a practical three-stage procedure is proposed for the empirical estimation of plausible  $K$  and  $\epsilon$  values, and finding a clue about a potential ONL without undertaking extensive calculations:

4.1.2.1. Stage A: Finding a neighboring point to the target UPO. Since the only available information about the target UPO is its period, first a state space location close enough to a period- $T$  UPO needs to be found, to be used at the next stages. At this stage, first the system (either real or simulation experiment) is run long enough ( $T_{\text{run}}$ ) in an uncontrolled manner while recording  $\|\Delta_{\mathbf{T}}(t)\|$ . Based on the fact that

$\|\Delta_{\mathbf{T}}(t)\|$  will be relatively small when the system is close enough to a period-T UPO, the recorded data are scanned to find  $t^*$  that minimizes  $\|\Delta_{\mathbf{T}}(t)\|$ . (See Figure 4.2, which shows  $\|\Delta_{\mathbf{T}}(t)\|$  as a function of time for  $T = 5.89$  of the uncontrolled Rössler system.)

$$\|\Delta_{\mathbf{T}}(t)\|_{min} = \|\Delta_{\mathbf{T}}(t^*)\| = \|\mathbf{x}(t^*) - \mathbf{x}(t^* - T)\| \quad (4.4)$$

Here,  $\mathbf{x}(t^* - T)$  is a state that is the closest to a period-T UPO and keeps approaching the UPO under the uncontrolled system dynamics.  $\mathbf{x}^* = \mathbf{x}(t^* - T)$  will be used as the initial point at the next stage of the TAF procedure.

4.1.2.2. Stage B: Estimation of the control gain. At the next stage, the aim is to find a suitable control gain. For that purpose, starting from  $\mathbf{x}^*$ , the system is run for a given duration  $T_{run} \gg T$ , applying TAF control in an unrestricted manner (i.e. without imposing the  $\|\Delta_{\mathbf{T}}(t)\| < \epsilon$  criterion) with different control gains  $K \in \mathbf{R}_K$  (a reasonable range of control gains). At each run with a given  $K$ , the rms value of the tail aperture vector  $\|\Delta_{\mathbf{T}}(t)\|_{rms}$  is calculated as follows (as used by Pyragas in [10])

$$\|\Delta_{\mathbf{T}}(t)\|_{rms} = \sqrt{\frac{1}{T_{run}} \int_{\tau=0}^{T_{run}} \|\Delta_{\mathbf{T}}(\tau)\|^2 d\tau} \quad (4.5)$$

The control gain value, which makes  $\|\Delta_{\mathbf{T}}(t)\|_{rms}$  minimum, is chosen as a candidate gain  $K_{cand}^*$  (see Figure 4.3, which shows  $\|\Delta_{\mathbf{T}}(t)\|_{rms}$  as a function of different control gain values for  $T = 5.89$  in a chaotic Rössler system).

In order to check whether a TAF controller with  $K_{cand}^*$  indeed stabilizes the target UPO, the system is run under unrestricted TAF control with  $K_{cand}^*$  for a duration  $T_{run} \gg T$  starting from  $\mathbf{x}^*$ . If the controller fulfills its purpose, the system that has started at  $\mathbf{x}^*$  close enough to the target UPO will stay close enough for the rest of the time. In this thesis, the average flow magnitude along the target UPO (passing close to  $\mathbf{x}^*$  and having period  $T$ ) is proposed as a characteristic of the system's behavior

on the target UPO<sup>2</sup>. This scalar characteristic value  $\langle \|\dot{\mathbf{x}}\| \rangle_{uncont}$  can be estimated from the results of Stage A, where the uncontrolled system has been found to travel temporarily close enough to the target UPO between  $(t^* - T)$  and  $t^*$ :

$$\langle \|\dot{\mathbf{x}}\| \rangle_{uncont} = \frac{1}{T} \int_{\tau=t^*-T}^{t^*} \|\dot{\mathbf{x}}(\tau)\| d\tau \quad (4.6)$$

The performance of the control with  $K_{cand}^*$  can be assessed by comparing a long-term average of the flow magnitudes  $\langle \|\dot{\mathbf{x}}\| \rangle_{test}$ ,

$$\langle \|\dot{\mathbf{x}}\| \rangle_{test} = \frac{1}{mT} \int_{\tau=T_{run}-mT}^{T_{run}} \|\dot{\mathbf{x}}(\tau)\| d\tau \quad (4.7)$$

where  $T_{run} \gg mT$ ,  $m$  is a small integer and  $\|\dot{\mathbf{x}}(\tau)\|$  is the flow magnitude under the application of the unrestricted TAF control with  $K_{cand}^*$ . It should be noted that the absence of the restriction on the magnitude of the control input does not make any difference because if the controller is successful, the system that starts from  $\mathbf{x}^*$  will always remain close to the target UPO such that the magnitude of the control input will anyway be below the threshold. If  $\langle \|\dot{\mathbf{x}}\| \rangle_{test}$  turns out to be close enough to  $\langle \|\dot{\mathbf{x}}\| \rangle_{uncont}$ , it is concluded that  $K_{cand}^*$  indeed stabilizes a period- $T$  UPO and thus  $K_{cand}^*$  can be taken as  $K^*$  (see Figure 4.4). If this condition is not satisfied, this can be considered as an indicator of the possibility of an Odd Number Limitation (ONL). Although, not exactly a proof of ONL, this relatively simple test provides a practical way for suspecting ONL without extensive calculations or exact prior knowledge about the system.

4.1.2.3. Stage C: Estimation of an appropriate tail aperture tolerance. Since TAF control proposed in this thesis, is based on the principle of keeping the control input bounded (both in order to save energy and to avoid alteration of the chaotic system characteristics far from the target UPO), a practical way of estimating a plausible threshold value  $\epsilon^*$  is needed. As a matter of fact, the control input is kept bounded by

---

<sup>2</sup>The average flow magnitude along the target UPO can be considered as a signature of the target UPO. Hypothetically, it is possible that there exist other trajectories that have a similar signature, but this is highly improbable.

applying control only when  $\|\Delta_{\mathbf{T}}(t)\|$  is small enough. The average of the local minima of  $\|\Delta_{\mathbf{T}}(t)\|$  obtained from the uncontrolled system run in stage A can be used as a reasonable heuristic estimate for  $\epsilon^*$  (see Figure 4.2, where  $\|\Delta_{\mathbf{T}}(t)\|$  is given as a function of time and the red line corresponds to the tail aperture tolerance  $\epsilon^*$  for period-5.89 UPO of the Rössler system.).

### 4.1.3. Simulation Examples

The simulation results obtained by applying the proposed procedure of parameter estimation and the TAF control are presented for the Rössler and Lorenz systems below:

4.1.3.1. Rössler System. Consider a Rössler system described by the system equations:

$$\begin{aligned}\dot{x}_1 &= -x_2 - x_3 \\ \dot{x}_2 &= x_1 + 0.2x_2 \\ \dot{x}_3 &= 0.2 + x_3(x_1 - 5.7)\end{aligned}\tag{4.8}$$

Control Task: Stabilization of a UPO of the Rössler system with period  $T = 5.89$

*Stage A:* Find  $t^*$  such that  $\|\Delta_{\mathbf{T}}(t)\|_{min} = \|\Delta_{\mathbf{T}}(t^*)\|$  and obtain  $\mathbf{x}^*$  such that  $\mathbf{x}^* = \mathbf{x}(t^* - T)$  (Figure 4.2).

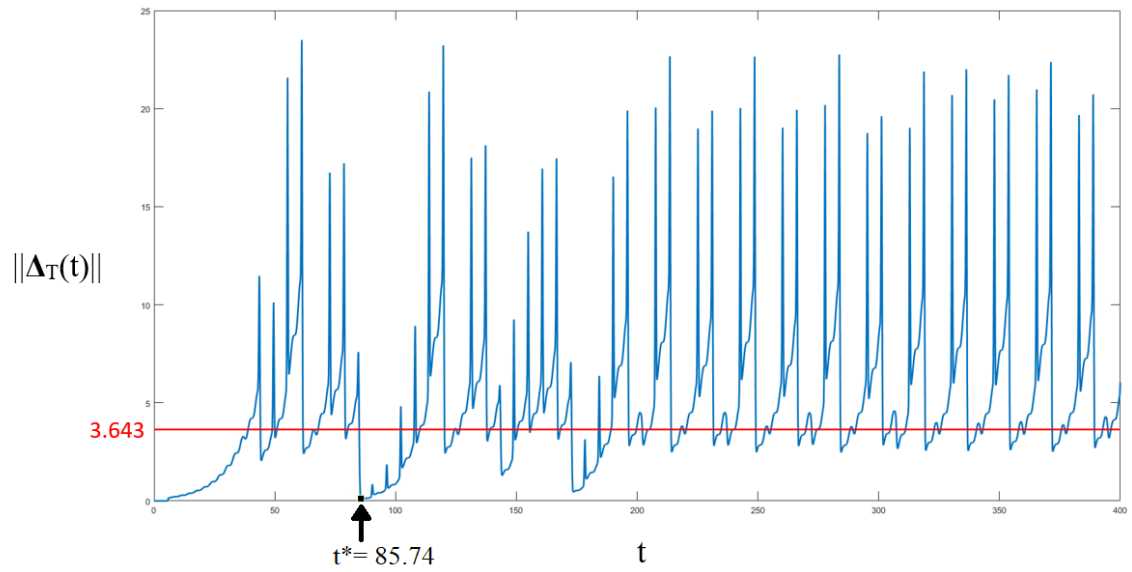


Figure 4.2.  $\|\Delta_{5.89}(t)\|$  as a function of time for an uncontrolled Rössler system, here, the red line expresses the average of the local minima  $\epsilon^* = 3.643$ ,  $t^* = 85.74$ ,

$$\|\Delta_{\mathbf{T}}(t^*)\| = 0.1146, \text{ and } \mathbf{x}^* = \mathbf{x}(t^* - T)$$

*Stage B:* Obtain  $K_{\text{cand}}^*$ , which minimizes  $\log_{10} \|\Delta_{\mathbf{T}}(t)\|_{\text{rms}}$  (Figure 4.3).

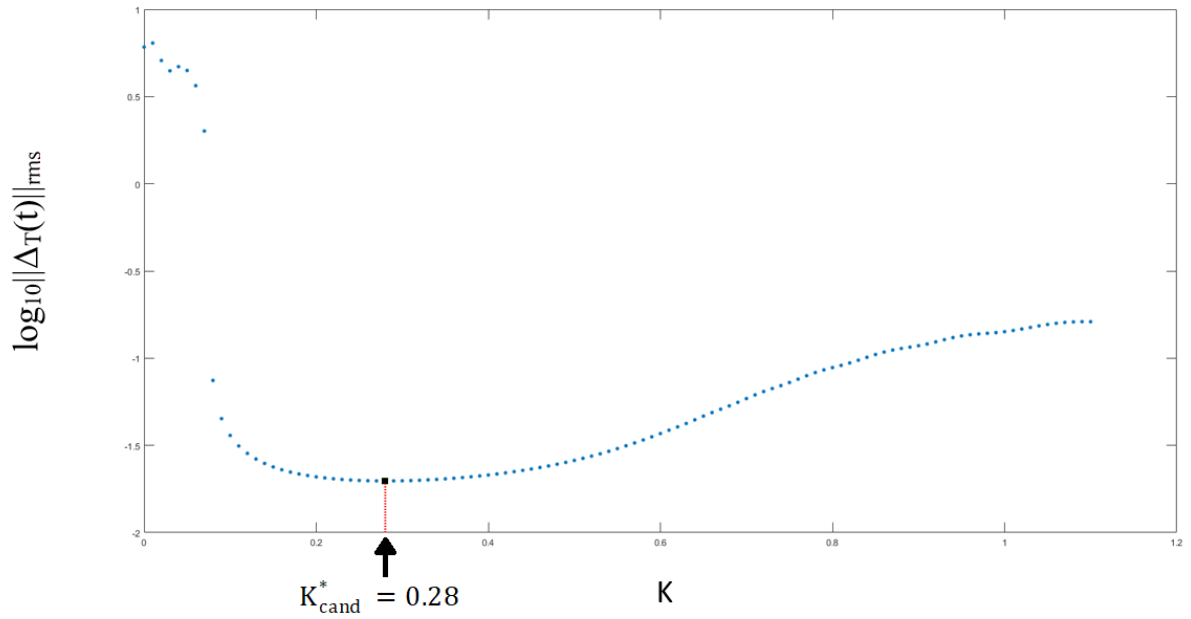


Figure 4.3.  $\log_{10} \|\Delta_{\mathbf{T}}(t)\|_{rms}$  as a function of  $K$  in Rössler system for  $T = 5.89$ , where  $K_{cand}^* = 0.28$ .

Test the performance of the unrestricted TAF control with  $K_{cand}^*$  (Figure 4.4).

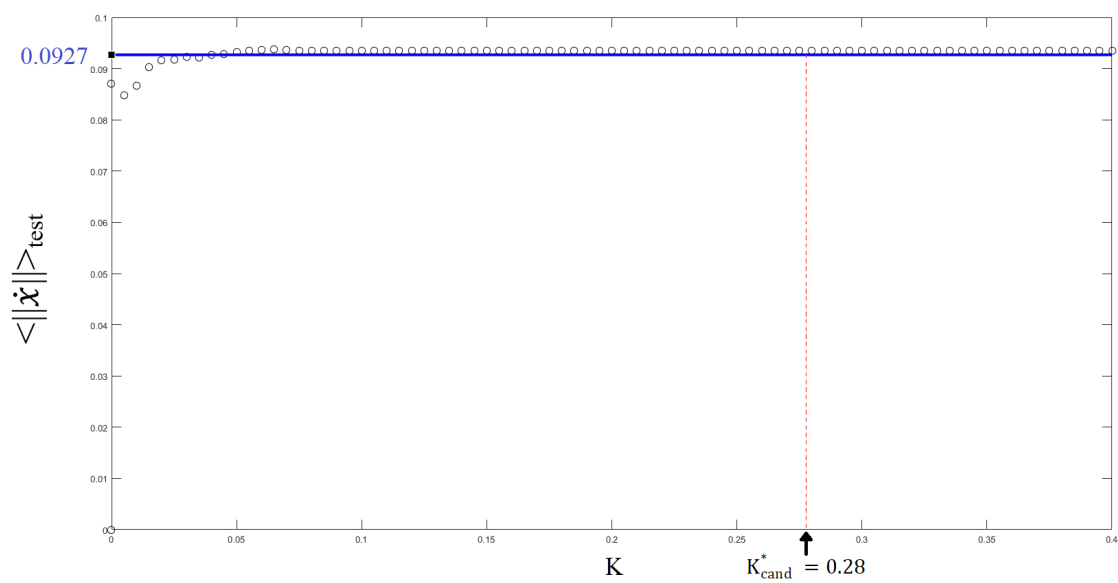


Figure 4.4.  $\langle \|\dot{\mathbf{x}}\| \rangle_{test}$  as a function of  $K$ , here the blue line illustrates  $\langle \|\dot{\mathbf{x}}\| \rangle_{uncont} = 0.0927$ .

It is observed from Figure 4.4 that  $\langle \|\dot{\mathbf{x}}\| \rangle_{test}$  obtained with  $K_{cand}^* = 0.28$  is close enough to  $\langle \|\dot{\mathbf{x}}\| \rangle_{uncont} = 0.0927$  (4.6), thus  $K_{cand}^*$  can be used as the TAF control gain  $K^*$ .

*Stage C:*

The average of local minima of  $\|\Delta_{\mathbf{T}}(t)\|$  in Figure 4.2 for the period-5.89 UPO of Rössler system has been obtained as 3.643, thus the tail aperture tolerance can be chosen as  $\epsilon^* = 3.643$ . According to the proposed three stage procedure above, the estimated parameters have been found as  $K_{cand}^* = 0.28$  and  $\epsilon^* = 3.643$ . The TAF method with these parameters has successfully stabilized the target UPO. Figure 4.5, Figure 4.6 and Figure 4.7 show the results of stabilization of the UPO with period 5.89 of the Rössler system.

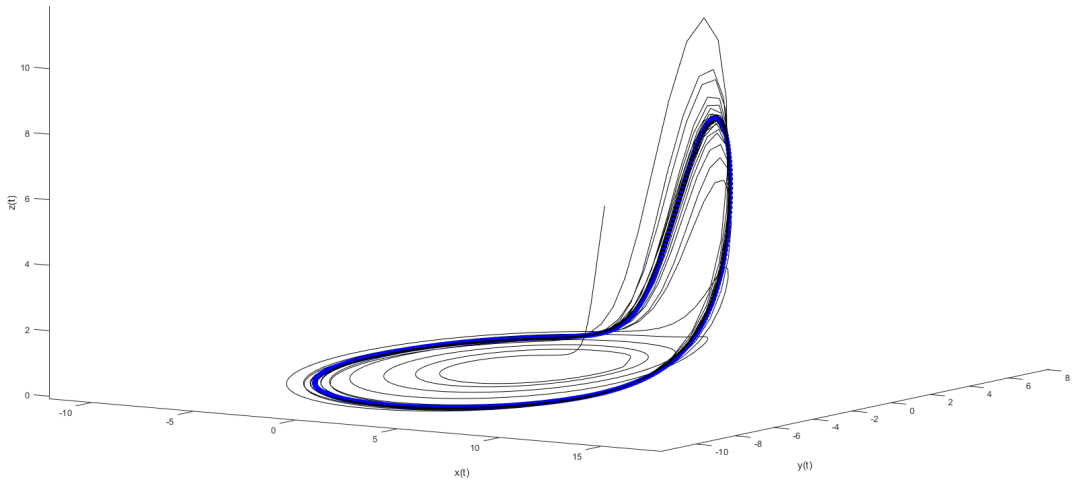


Figure 4.5. Stabilized period-5.89 UPO of the Rössler system .

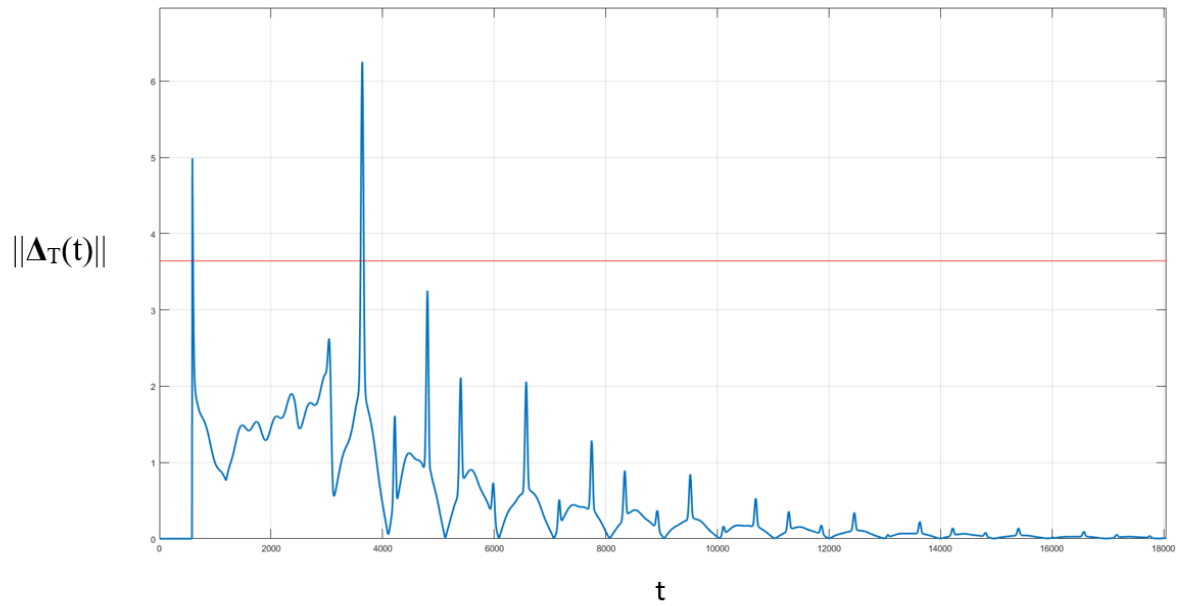


Figure 4.6.  $\|\Delta_{5.89}(t)\|$  as a function of time under the control of the TAF method with  $K_{\text{cand}}^* = 0.28$  and  $\epsilon^* = 3.643$ .

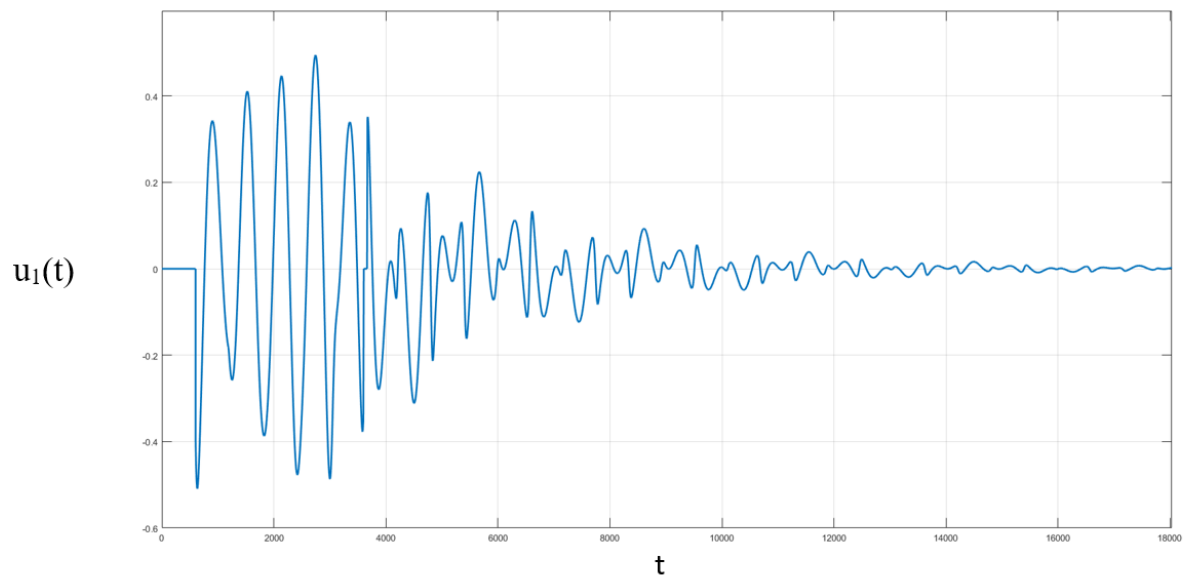


Figure 4.7. The first component of the input vector as a function of time under the control of the TAF method with  $K_{\text{cand}}^* = 0.28$  and  $\epsilon^* = 3.643$ .

4.1.3.2. Lorenz System. Consider a Lorenz system described by the system equations:

$$\begin{aligned}\dot{x}_1 &= 10(x_2 - x_1) \\ \dot{x}_2 &= x_1(28 - x_3) - x_2 \\ \dot{x}_3 &= x_1x_2 - \frac{8}{3}x_3\end{aligned}\tag{4.9}$$

Control Task: Stabilization of a UPO of the Lorenz system with period  $T = 1.56$ . In the literature, this UPO is known to have Odd Number Limitation (ONL) because of the single unstable Floquet multiplier  $\mu \approx 4.713$  [21].

*Stage A:* Find  $t^*$  such that  $\|\Delta_{\mathbf{T}}(t)\|_{min} = \|\Delta_{\mathbf{T}}(t^*)\|$  and obtain  $\mathbf{x}^*$  such that  $\mathbf{x}^* = \mathbf{x}(t^* - T)$  (Figure 4.8).

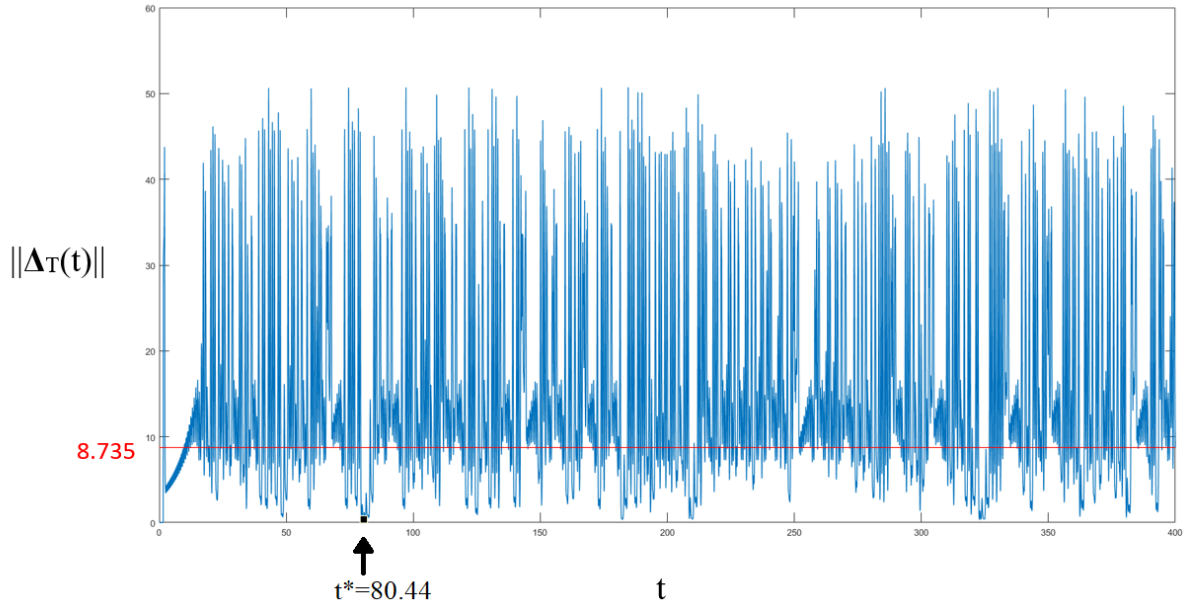


Figure 4.8.  $\|\Delta_{1.56}(t)\|$  as a function of time for an uncontrolled Lorenz system, here, the red line expresses the average of the local minima  $\epsilon^* = 8.735$ ,  $t^* = 80.44$ ,

$$\|\Delta_{\mathbf{T}}(t^*)\| = 0.3484, \text{ and } \mathbf{x}^* = \mathbf{x}(t^* - T)$$

*Stage B:* Obtain  $K_{\text{cand}}^*$ , which minimizes  $\log_{10} \|\Delta_{\mathbf{T}}(t)\|_{rms}$  (Figure 4.9).

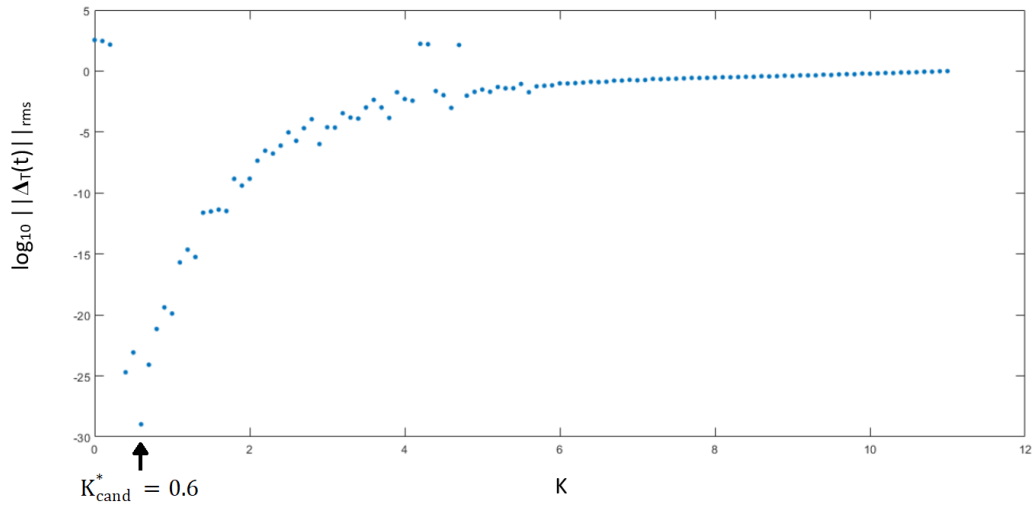


Figure 4.9.  $\log_{10} \|\Delta_{\mathbf{T}}(t)\|_{rms}$  as a function of  $K$  in Lorenz system for  $T = 1.56$  where  $K_{cand}^* = 0.6$ .

Test the performance of the unrestricted TAF control with  $K_{cand}^*$  (Figure 4.10).

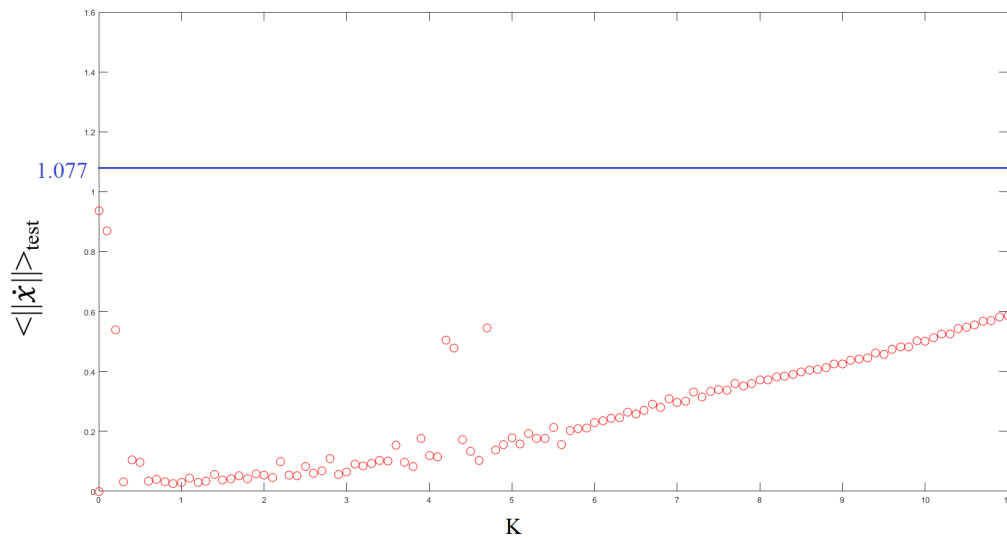


Figure 4.10.  $\langle \|\dot{\mathbf{x}}\| \rangle_{test}$  as a function of  $K$ , here the blue line illustrates  $\langle \|\dot{\mathbf{x}}\| \rangle_{uncont} = 1.077$ .

In Figure 4.9, the minimum around  $K_{\text{cand}}^* = 0.6$  seems to accomplish the stabilization of the target UPO with  $T = 1.56$ . However, as seen from Figure 4.10, this is misleading, because actually what is stabilized is another equilibrium behavior which satisfies  $\mathbf{x}(t) = \mathbf{x}(t - T)$  (a UPO with period  $T/k$ , which can also be an equilibrium point when  $k \rightarrow \infty$ ).

In the Lorenz system considered here,  $K_{\text{cand}}^* = 0.6$  cannot be used as a control gain of TAF method for the stabilization of the period-1.56 UPO. Thus, there is no need to proceed to Stage C. This example of the Lorenz system indicates that the TAF method cannot stabilize the 1.56-periodic target UPO, which is known to have Odd Number Limitation (ONL).

## 4.2. TAF with Sparsification

As can be concluded from the procedure described in the previous section, and can be observed from 4.1, the TAF control method has the advantage of computational simplicity and of having a minimal requirement on prior knowledge (only the period of the target UPO), while sharing with all other delayed feedback-based methods the burden of keeping track of the system trajectory during the last  $T$  units of time.

The TAF control is active only when the tail aperture magnitude ( $\|\Delta_{\mathbf{T}}(t)\|$ ) is below a certain tolerance  $\epsilon^*$ , which means that the system is momentarily behaving in an almost  $T$ -periodic manner. Hence, the task of the controller can be considered as maintaining the  $T$ -periodic behavior, whenever the system is close to it. Given this inherent tolerance of the TAF control method, it may be meaningful to reduce the number of data points to be stored, i.e. reduce the sampling rate, provided that the distance between the data points does not exceed a reasonable fraction of  $\epsilon^*$ . Let us call this fraction  $k_{\text{th}}$ , the sparsification factor, and propose a nonuniform sampling algorithm that amounts to the sparsification of the trajectory data such that data points that are closer to each other than  $\frac{\epsilon^*}{k_{\text{th}}}$  are not stored (Figure 4.11).

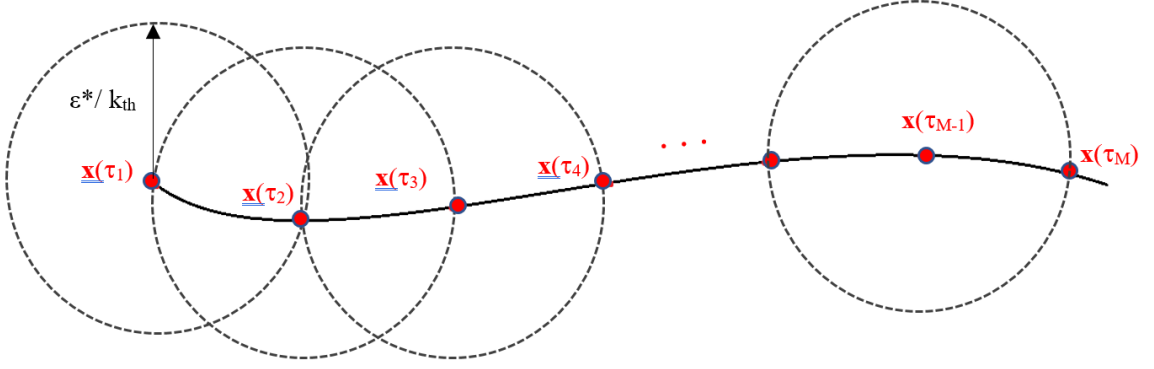


Figure 4.11. Filling the time and state registers in the sparsification algorithm

The sparsed trajectory data consists of two linked sequences: a sequence of registered time instants  $\{\tau_1, \dots, \tau_M\}$  and a sequence of registered states  $\{\mathbf{x}_1, \dots, \mathbf{x}_M\}$ , which can be generated and updated in an online manner according to the following procedure as time flows starting from  $t = 0$ . The procedure can be considered in two stages:

#### 4.2.1. Stage 1: Filling the registers

Initiate the registers with  $\tau_1 = 0$  and  $\mathbf{x}(\tau_1) = 0$ . Add new entries to the registers according to the following iterative rule where  $t_{\text{reg}1}$ ,  $t_{\text{reg}2}$  and  $t_{\text{reg}M}$  are the first, second and the last element of the time register, respectively:

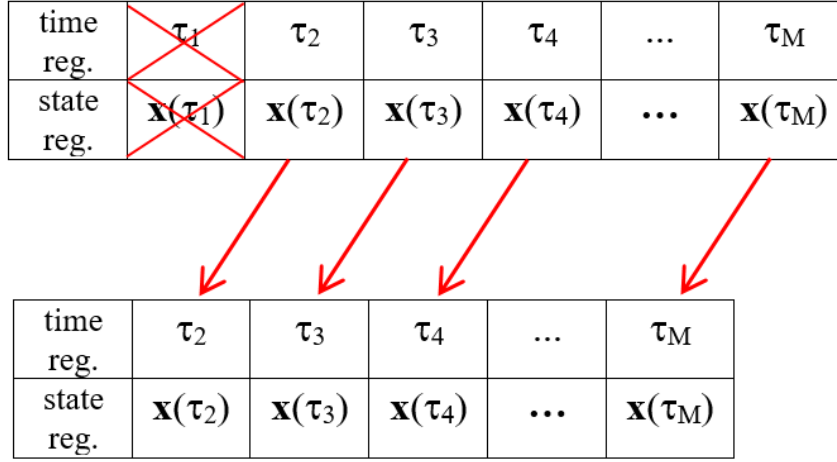
$$\text{For } t > \tau_i : \text{ if } \|\mathbf{x} - \mathbf{x}_i\| > \frac{\epsilon^*}{k_{\text{th}}} \implies \tau_{i+1} = t; \quad \mathbf{x}_{i+1} = \mathbf{x}(\tau_{i+1})$$

$$\text{if } (t_{\text{reg}M} - t_{\text{reg}1}) > T \quad \text{and} \quad (t_{\text{reg}M} - t_{\text{reg}2}) > T \implies \text{go to Stage 2}$$

<b>time reg.</b>	$\tau_1$	$\tau_2$	$\tau_3$	$\tau_4$	...
<b>state reg.</b>	$\mathbf{x}_1 = \mathbf{x}(\tau_1)$	$\mathbf{x}_2 = \mathbf{x}(\tau_2)$	$\mathbf{x}_3 = \mathbf{x}(\tau_3)$	$\mathbf{x}_4 = \mathbf{x}(\tau_4)$	...

#### 4.2.2. Stage 2: Updating the registers

Discard the first entries of the sequences, shift the registers towards left. After updating the registers as shown below, continue to Stage 1.



TAF control cannot be activated in Stage 1 because past data for a duration of one period has not yet been accumulated. In Stage 2, when the TAF control is activated, at any time instant  $t$ , the system state at  $(t - T)$  will be needed for the calculation of  $\Delta_T(t)$ . However, the registers will most of the time not contain any data that exactly corresponds to  $(t - T)$ . In such cases,  $\mathbf{x}(t - T)$  can be estimated by linear interpolation between data points corresponding to  $\tau_i$  and  $\tau_{i+1}$ , where  $\tau_i < (t - T) < \tau_{i+1}$ , as follows:

$$\mathbf{x}_{est}(t - T) = \mathbf{x}_i + \frac{\mathbf{x}_{i+1} - \mathbf{x}_i}{\tau_{i+1} - \tau_i}(t - T - \tau_i) \quad (4.10)$$

For the sake of clarity, an explanatory example for the proposed data reduction algorithm is given below.

e.g. Let's assume  $T=2$ .

Initial point:

time reg.	0
state reg.	$\mathbf{x}(0)$

2<sup>nd</sup> update:

time reg.	0	1
state reg.	$\mathbf{x}(0)$	$\mathbf{x}(1)$

3<sup>rd</sup> update:

time reg.	0	1	1.2
state reg.	$\mathbf{x}(0)$	$\mathbf{x}(1)$	$\mathbf{x}(1.2)$

4<sup>th</sup> update:

time reg.	0	1	1.2	2.5
state reg.	$\mathbf{x}(0)$	$\mathbf{x}(1)$	$\mathbf{x}(1.2)$	$\mathbf{x}(2.5)$

5<sup>th</sup> update:

time reg.	<del>0</del>	1	1.2	2.5	3.2
state reg.	<del><math>\mathbf{x}(0)</math></del>	$\mathbf{x}(1)$	$\mathbf{x}(1.2)$	$\mathbf{x}(2.5)$	$\mathbf{x}(3.2)$

Since  $(t_{\text{regM}} - t_{\text{regM}}) = 3.2 - 0 = 3.2 > T$  and  $(t_{\text{regM}} - t_{\text{reg2}}) = 3.2 - 1 = 2.2 > T$ , the sequences will be shifted towards left as seen below.

<b>time reg.</b>	1	1.2	2.5	3.2
<b>state reg.</b>	$\mathbf{x}(1)$	$\mathbf{x}(1.2)$	$\mathbf{x}(2.5)$	$\mathbf{x}(3.2)$

The proposed sparsification approach allows the controller to work in a lower resolution mode which reduces memory usage by decreasing the total data stored as investigated in Table 4.4.

### 4.3. Performance Evaluation of TAF

As can be seen from the simulation examples in Section 4.1, by using the chosen parameters ( $K^*$  and  $\epsilon^*$ ), the TAF method can successfully stabilize UPOs of chaotic systems that have no ONL (see: Figure 4.5 and Figure 4.6). Furthermore, in case of ONL, (at least in the tested examples) our method turned out to be successful in finding an indication about ONL in early stages of the procedure without extensive calculations or prior knowledge (see: Figure 4.10).

Table 4.1. Main aspects of the best known chaos control methods applicable to continuous time systems

Method	Control	Necessary prior knowledge	Challenges & Limitations	Research
Delayed Feedback Control (DFC)	<p><u>Control input:</u> Additive</p> <p><u>Control Law:</u>  <math>u(t) = K(y(t-T)-y(t))</math>            where <math>y = g(\mathbf{x})</math> is a measurable scalar output</p>	Period T of the target UPO	<ul style="list-style-type: none"> <li>• Difficulty to stabilize UPOs with large Floquet Multipliers (remediation: EDFC [26])</li> <li>• ONL</li> </ul>	(Pyragas, K., 1992) [10]
Proportional Feedback Control (PFC)	<p><u>Control input:</u> Additive</p> <p><u>Control Law:</u>  <math>u(t) = K[\mathbf{x}^*(t)-\mathbf{x}(t)]</math></p>	$\{\mathbf{x}^*(\tau), 0 \leq \tau < T\}$ Description of the target UPO	<ul style="list-style-type: none"> <li>• Computational &amp; practical difficulty</li> </ul>	(Pyragas, K., 1992) [10]
Tail Aperture Feedback (TAF)	<p><u>Control input:</u> Additive</p> <p><u>Control Law:</u>  <math>u(t) = K[\mathbf{x}(t-T)-\mathbf{x}(t)]</math></p>	Period T of the target UPO	<ul style="list-style-type: none"> <li>• ONL</li> <li>• Storing data for the last period (remediation: Sparsification)</li> </ul>	Proposed in this thesis
OGY Control	<p><u>Control input:</u> Perturbations of some control parameter</p> <p><u>Control Law:</u>            Local linear control at discrete time instances when the system trajectory traverses the chosen Poincaré surface</p>	The location $\xi^*$ , where the target UPO traverses the Poincaré surface	<ul style="list-style-type: none"> <li>• Difficulty to stabilize UPOs with large Floquet Multipliers</li> <li>• Limitation of the control update to Poincaré surface traversals</li> </ul>	(Ott, E., C. Grebogi and J. A. Yorke, 1990) [5]
Prediction Based Control (PBC)	<p><u>Control input:</u> Additive</p> <p><u>Control Law:</u>  <math>u(t) = K(\phi(t+T, t, \mathbf{x}(t), 0) - \mathbf{x}(t))</math></p>	System Equations	<ul style="list-style-type: none"> <li>• Computational &amp; practical difficulty</li> </ul>	(T. Ushio and S. Yamamoto, 1999) [25]

A summary of the main aspects of various chaos control methods used for the stabilization of a target UPO of a continuous time chaotic system is shown in Table 4.1. Since the operating conditions of most of these methods are different than those of TAF control, in this thesis, only a comparison of the TAF method and the DFC method has been investigated, taking the output  $\mathbf{y}(t) = \mathbf{x}(t)$  in the DFC method, for the sake of fair comparison.

#### 4.3.1. Comparison of the original DFC and the TAF method

Here, the TAF and DFC methods are compared according to two performance criteria: stabilization time and control power expenditure. For the sake of fair comparison the full-state version ( $\mathbf{y}(t) = \mathbf{x}(t)$ ) of the DFC method is used (as opposed to [11]). These are shown in Table 4.2 and 4.3 for UPOs of the Rössler system with  $T=17.5$  and  $T=35.01$ , respectively.

The stabilization time  $\hat{t}_{st}$  is the time it takes for the controller to stabilize the target UPO, starting from an arbitrary initial condition. It can be calculated as the average of  $t_{st}$ 's obtained for many different initial conditions, where  $t_{st}$  is defined as  $\min t_{st}: \|\Delta_{\mathbf{T}}(t)\| < \epsilon^* \quad \forall t \geq t_{st}$ .

The control power expenditure  $\hat{P}_{rms}$  can be similarly calculated as the rms value of the control input, averaged over many different initial conditions. Below,  $\hat{P}_{rms}$  and  $\hat{t}_{st}$  obtained by averaging results for 20 different initial conditions.

Table 4.2. Comparison of the TAF and DFC methods applied to a chaotic Rössler system with  $T = 17.5$  and  $K = 0.2$  ( $\hat{t}_{st}$  calculated according to the same  $\epsilon^*$  for both methods)

<b>Rössler System</b>	Tail aperture tolerance, $\epsilon^*$	Control power expenditure, $\hat{P}_{rms}$	Stabilization time, $\hat{t}_{st}$
<b>DFC, [10]</b>	not in use	0.0466	43.9
<b>TAF, [this thesis]</b>	1.6576	0.0422	31.2

Table 4.3. Comparison of the TAF and DFC methods applied to a chaotic Rössler system with  $T = 35.01$  and  $K = 0.9$  ( $\hat{t}_{st}$  calculated according to the same  $\epsilon^*$  for both methods)

<b>Rössler System</b>	Tail aperture tolerance, $\epsilon^*$	Control power expenditure, $\hat{P}_{rms}$	Stabilization time, $\hat{t}_{st}$
<b>DFC, [10]</b>	not in use	0.0685	151.7
<b>TAF, [this thesis]</b>	2.09	0.0208	85.65

As can be seen from Table 4.2 and 4.3, the TAF method expends less than the DFC method, which is expected, because the confinement of the control activity to  $\|\Delta_{\mathbf{T}}(t)\| < \epsilon^*$  puts a radical bound on it. The superiority of TAF in terms of the stabilization time comes as a surprise, and can be interpreted as an indicator of the fact that control efforts far from the target UPO interfere with the natural behavior of the chaotic system and prolong the approach to the close neighborhood of the target UPO.

#### 4.3.2. Comparison of the TAF method with and without Sparsification

In Table 4.4, the effects of sparsification factor  $k_{th}$  on the performance of the TAF controller is given, where the performance criteria are the average data stored and the quality of stabilization for the 5.89-periodic UPO of the Rössler system with  $K^* = 0.28$  and  $\epsilon^* = 3.643$  (as found in Section 4.1.3). It should be noted that the quality of stabilization is expressed in terms of the time average of  $\|\Delta_{\mathbf{T}}(t)\|$ .

Table 4.4. The dependence of the average size of stored data and of the quality of stabilization on the sparsification factor  $k_{th}$

Method	$k_{th}$	$\varepsilon^*/k_{th}$	Average data stored per unit time	Time average of $\ \Delta_T(t)\ $ (quality of stabilization)
TAF without Data Reduction	-	-	585	0.0092
TAF with Data Reduction	8	0.455	109	0.0319
TAF with Data Reduction	4	0.910	58	0.0322
TAF with Data Reduction	2	1.820	31	0.0437
TAF with Data Reduction	1	3.643	16	0.2666

As expected, smaller  $k_{th}$  results in less data storage, while it degrades the quality of stabilization due to the approximation errors resulting from the interpolation between registered data points.

## 5. DISCUSSION AND CONCLUSION

In this thesis delayed feedback-based approaches to chaos control in continuous-time systems have been investigated, and a new delayed feedback-based chaos control method has been developed together with a practical procedure for the empirical estimation of adequate parameter values to be used in the controller. This new method, which has been dubbed the Tail Aperture Feedback (TAF) method combines the basic DFC approach with some ideas borrowed from the OGY type chaos control. As such, TAF control can be considered as an improved version of the original DFC method applicable under the assumption that the full-state vector is observable. Therefore, it shares DFC's advantage of requiring minimal a priori knowledge about the system (only the period of the target UPO), while offering the additional advantages of (i) computational simplicity, (ii) shorter stabilization time, (iii) lower control power expenditure, and (iv) the ability to sense the presence of Odd Number Limitation (ONL) without undertaking extensive calculations. This last ability is provided by a criterion proposed in this thesis as a measure of the quality of stabilization of the target UPO.

The restrictions of this method are the assumptions about the observability of the full-state and the possibility of applying additive control on all states. The TAF method also requires that the controller is able to store the system trajectory for the last  $T$  units of time (period of the target UPO). To alleviate this memory requirement, a practical sparsification method has been proposed, which can be implemented in an online manner.

The efficacies of the TAF control, the ONL estimation method, and the sparsification method have been demonstrated via simulations of Lorenz and Rössler systems.

Future investigations may relax the fundamental assumption of the TAF control about the observability of the full system state if it can be combined with an appropriate observer design.

## REFERENCES

1. Lorenz, E. N., “Deterministic Nonperiodic Flow”, *Journal of the Atmospheric Sciences*, Vol. 20, pp. 130–141, 1963.
2. Li, T.-Y. and J. A. Yorke, “Period three implies chaos”, *The American Mathematical Monthly*, Vol. 82, No. 10, pp. 985–992, 1975.
3. Cantor, G., “Über unendliche, lineare Punktmannigfaltigkeiten”, *Mathematische Annalen*, Vol. 21, No. 5, pp. 545–586, 1883.
4. Mandelbrot, B. B., *The fractal geometry of nature*, W.H. Freeman, San Francisco, 1982.
5. Strogatz, S. H., *Nonlinear dynamics and chaos: with applications to physics, biology, chemistry, and engineering*, Westview press, 2014.
6. Ott, E., C. Grebogi and J. A. Yorke, “Controlling chaos”, *Physical review letters*, Vol. 64, No. 11, p. 1196, 1990.
7. Barreto, E. and C. Grebogi, “Multiparameter control of chaos”, *Physical Review E*, Vol. 52, No. 4, p. 3553, 1995.
8. Iplikci, S. and Y. Denizhan, “Targeting in dissipative chaotic systems: A survey”, *Chaos: An Interdisciplinary Journal of Nonlinear Science*, Vol. 12, No. 4, pp. 995–1005, 2002.
9. Dressler, U. and G. Nitsche, “Controlling chaos using time delay coordinates”, *Physical Review Letters*, Vol. 68, No. 1, p. 1, 1992.
10. de Paula, A. S. and M. A. Savi, “A multiparameter chaos control method based on OGY approach”, *Chaos, Solitons & Fractals*, Vol. 40, No. 3, pp. 1376–1390, 2009.

11. Pyragas, K., “Continuous control of chaos by self-controlling feedback”, *Physics Letters A*, Vol. 170, No. 6, pp. 421–428, 1992.
12. Tian, Y., J. Zhu and G. Chen, “A survey on delayed feedback control of chaos”, *Journal of Control Theory and Applications*, Vol. 3, No. 4, pp. 311–319, 2005.
13. Pyragas, K., “Delayed feedback control of chaos”, *Philosophical Transactions of the Royal Society A: Mathematical, Physical and Engineering Sciences*, Vol. 364, No. 1846, pp. 2309–2334, 2006.
14. Pyragas, K., “A twenty-year review of time-delay feedback control and recent developments”, *International Symposium on Nonlinear Theory and its Applications*, Vol. 1, pp. 683–686, 2012.
15. Kuznetsov, N. V., G. A. Leonov and M. M. Shumafov, “A short survey on Pyragas time-delay feedback stabilization and odd number limitation”, *IFAC-PapersOnLine*, Vol. 48, No. 11, pp. 706–709, 2015.
16. Socolar, J. E. S., D. W. Sukow and D. J. Gauthier, “Stabilizing unstable periodic orbits in fast dynamical systems”, *Physical Review E*, Vol. 50, No. 4, pp. 3245–3248, 1994.
17. Pyragas, K., “Control of chaos via extended delay feedback”, *Physics Letters A*, Vol. 206, No. 5-6, pp. 323–330, 1995.
18. Ushio, T., “Limitation of delayed feedback control in nonlinear discrete-time systems”, *IEEE Transactions on Circuits and Systems I: Fundamental Theory and Applications*, Vol. 43, No. 9, pp. 815–816, 1996.
19. Nakajima, H., “On analytical properties of delayed feedback control of chaos”, *Physics Letters A*, Vol. 232, No. 3-4, pp. 207–210, 1997.
20. Just, W., T. Bernard, M. Ostheimer, E. Reibold and H. Benner, “Mechanism of

- Time-Delayed Feedback Control”, *Physical Review Letters*, Vol. 78, No. 2, pp. 203–206, 1997.
21. Morgül, m., “On the stability of delayed feedback controllers”, *Physics Letters A*, Vol. 314, No. 4, pp. 278–285, 2003.
  22. Fiedler, B., V. Flunkert, M. Georgi, P. Hövel and E. Schöll, “Refuting the Odd-Number Limitation of Time-Delayed Feedback Control”, *Physical Review Letters*, Vol. 98, No. 11, 2007.
  23. Hooton, E. W. and A. Amann, “Analytical Limitation for Time-Delayed Feedback Control in Autonomous Systems”, *Physical Review Letters*, Vol. 109, No. 15, 2012.
  24. Pyragas, K. and V. Novičenko, “Time-delayed feedback control design beyond the odd-number limitation”, *Physical Review E*, Vol. 88, No. 1, 2013.
  25. Dingwell, J. B., “Lyapunov exponents”, *Wiley encyclopedia of biomedical engineering*, 2006.
  26. Ushio, T. and S. Yamamoto, “Prediction-based control of chaos”, *Physics Letters A*, Vol. 264, pp. 30–35, 1999.
  27. Yamasue, K., K. Kobayashi, H. Yamada, K. Matsushige and T. Hikiyara, “Controlling chaos in dynamic-mode atomic force microscope”, *Physics Letters A*, Vol. 373, No. 35, pp. 3140–3144, 2009.
  28. Simmendinger, C. and O. Hess, “Controlling delay-induced chaotic behavior of a semiconductor laser with optical feedback”, *Physics Letters A*, Vol. 216, No. 1-5, pp. 97–105, 1996.
  29. Hikiyara, T. and T. Kawagoshi, “Experimental stabilization of unstable periodic orbit in magneto-elastic chaos by delayed feedback control”, *Chaos: An Interdisciplinary Journal of Nonlinear Science*, Vol. 12, No. 7, pp. 2837–2846, 1997.

30. Wolf, A., J. B. Swift, H. L. Swinney and J. A. Vastano, “Determining Lyapunov exponents from a time series”, *Physica D: Nonlinear Phenomena*, Vol. 16, No. 3, pp. 285–317, 1985.
31. Yang, C. and C. Q. Wu, “A robust method on estimation of Lyapunov exponents from a noisy time series”, *Nonlinear Dynamics*, Vol. 64, No. 3, pp. 279–292, 2011.
32. Nakajima, H. and Y. Ueda, “Half-period delayed feedback control for dynamical systems with symmetries”, *Physical Review E*, Vol. 58, No. 2, p. 1757, 1998.
33. Pyragas, K., “Control of Chaos via an Unstable Delayed Feedback Controller”, *Physical Review Letters*, Vol. 86, No. 11, pp. 2265–2268, 2001.
34. Slotine, J.-J. E. and W. Li, *Applied nonlinear control*, Prentice Hall, Englewood Cliffs, N.J, 1991.
35. Richards, J. A., *Analysis of periodically time-varying systems*, Springer Science & Business Media, 2012.

## APPENDIX A: DYNAMICAL SYSTEMS FUNDAMENTALS

In mathematics, dynamical systems are represented in terms of mathematical models which describe the change of the system states. More specifically, *continuous time systems* are represented by differential equations, while *discrete-time systems* are represented by difference equations. *Continuous time systems* can be represented in the general form as

$$\dot{\mathbf{x}}(t) = \mathbf{f}(\mathbf{x}(t), \mathbf{u}(t)) \quad (\text{A.1})$$

where  $\mathbf{x}(t) = [x_1(t), x_2(t), \dots, x_n(t)]^\top \in \mathbf{R}^n$  and  $\mathbf{u}(t) = [u_1(t), u_2(t), \dots, u_m(t)]^\top \in \mathbf{R}^m$  are the state and the input vectors, respectively, and  $\mathbf{f}$  is an  $n$ -dimensional vector function called the *system function*.

Linear systems is a special case of the general nonlinear systems of the form Equation A.1, where the system function  $\mathbf{f}$  is linear in the state and input variables. Thus, continuous-time linear dynamical systems can be represented as

$$\dot{\mathbf{x}}(t) = \mathbf{A}\mathbf{x}(t) + \mathbf{B}\mathbf{u}(t) \quad (\text{A.2})$$

where  $\mathbf{A}$  is an  $n \times n$  matrix and  $\mathbf{B}$  is an  $n \times m$  matrix,  $\mathbf{x}(t) \in \mathbf{R}^n$  represent the state vector and  $\mathbf{u}(t) \in \mathbf{R}^m$  represent the input vector, respectively.

An *equilibrium behavior* of a dynamical system is a behavior, which is sustained continuously in the absence of perturbations. *Equilibrium behaviors* can be subdivided into two such as static and dynamic ones. Static equilibrium behavior corresponds to the resting behavior at an equilibrium point, while dynamic equilibrium behavior include periodic motion on a closed orbit and the motion on a chaotic attractor. An

*equilibrium point*,  $\mathbf{x}^*$  has to satisfy Equation A.3.

$$\dot{\mathbf{x}}(t) = \mathbf{f}(\mathbf{x}(t)) = \mathbf{f}(\mathbf{x}^*) = \mathbf{0} \quad (\text{A.3})$$

A *periodic orbit* is a system behavior, where the system state repeats itself with a period  $T$ . A period- $T$  periodic orbit,  $\mathbf{x}^*(t)$ , of a continuous time system has to satisfy Equation A.4.

$$\mathbf{x}(t) = \mathbf{x}(t + T) = \mathbf{x}^*(t) \quad (\text{A.4})$$

Generally, the stability of an equilibrium behavior means that the system states that are close to the equilibrium behavior will remain close in the absence of perturbations. The asymptotic stability requires that system trajectories starting close to an equilibrium behavior asymptotically converge to the equilibrium behavior. Detailed definitions of stability can be found in Appendix B.

If the stability conditions are valid within the whole state space, the stability is said to be global, otherwise it is local. If a system has an attractor, the set of initial conditions which the system starts and converges to the attractor, is called the *basin of attraction* of that attractor.

Sensitivity to initial conditions implies that nearby trajectories diverge from each other which lead to a long term unpredictability.

Since continuous-time systems in a 2-D phase space cannot exhibit such dissipativeness and divergence of trajectories from each other without the states going to infinity, chaotic behavior can be observed in continuous-time systems only from 3-D onward. However, discrete-time systems can exhibit chaotic behavior even in 1-D.

The convergence/divergence behavior of nearby trajectories can be expressed in terms of Lyapunov exponents. An  $n$  dimensional system has  $n$  Lyapunov exponents corresponding to the exponential rate of divergence or convergence of nearby trajecto-

ries in the associated directions. Chaotic systems have at least one positive Lyapunov exponent indicating divergence in the associated direction and implying sensitivity to initial conditions. Detailed definitions for estimating *Lyapunov exponent* are given in [30, 31].

## APPENDIX B: STABILITY DEFINITIONS

The following definitions related to continuous-time systems are taken from [5,34]. Let us consider a dynamic system  $\dot{\mathbf{x}}(t) = \mathbf{f}(\mathbf{x}(t))$ .

**Definition B.1.** *An equilibrium point  $\mathbf{x}^*$  is said to be stable if, for any  $R > 0$ , there exists  $r > 0$ , such that if  $\|\mathbf{x}(0)\| < r$ , then  $\|\mathbf{x}(t)\| < R$  for all  $t > 0$ . Otherwise, the equilibrium point is unstable.*

**Definition B.2.** *An equilibrium point  $\mathbf{x}^*$  is asymptotically stable if it is stable, and in addition if there exists some  $r > 0$  such that  $\|\mathbf{x}(0)\| < r$  implies that for  $\mathbf{x}(t) \rightarrow 0$  as  $t \rightarrow \infty$ .*

**Definition B.3.** *An equilibrium point  $\mathbf{x}^*$  is exponentially stable if there exist two strictly positive numbers  $v$  and  $\lambda$  such that*

$$\forall t > 0, \|\mathbf{x}(t)\| < v\|\mathbf{x}(0)\|e^{-\lambda t}$$

*in some ball  $B_r$  around  $\mathbf{x}^*$ .*

**Definition B.4.** *If asymptotic (or exponential) stability holds for any initial states, the equilibrium point is said to be globally asymptotically (or exponentially) stable.*

### B.1. Linearization and Local Stability

Lyapunov's linearization method is concerned with the local stability of a nonlinear system. It is a formalization of the intuition that a nonlinear system should behave similarly to its linearized approximation for small range motions.

**Theorem B.5.** *Consider the linearization of the original nonlinear system in the equilibrium point  $\mathbf{x}^*$  as*

$$\dot{\mathbf{x}} = \mathbf{A}\mathbf{x} \tag{B.1}$$

where  $\mathbf{A}$  denote the Jacobian matrix of  $\mathbf{f}$  with respect to  $\mathbf{x}$  at  $\mathbf{x}^*$

$$A = \left( \frac{\partial \mathbf{f}}{\partial \mathbf{x}} \right)$$

Then,

- if all eigenvalues of  $A$  has negative real parts, then  $\mathbf{x}^*$  is asymptotically stable for the actual nonlinear system.
- If at least one of the eigenvalues of  $A$  has positive real part, then  $\mathbf{x}^*$  is unstable
- If all of the eigenvalues of  $A$  has negative real parts except at least one with zero real part, then no conclusion can be made for from the linear approximation.

## B.2. Lyapunov Stability Related Definitions and Theorems

The basic philosophy of Lyapunov's direct method is the mathematical extension of a fundamental physical observation: if the total energy of a mechanical (or electrical) system is continuously dissipated, then the system must eventually settle down to an equilibrium point. Thus, we may conclude the stability of a system by examining the variation of a single scalar function.

**Definition B.6.** A scalar continuous function  $V(\mathbf{x})$  is said to be locally positive definite if  $V(\mathbf{0}) = 0$  and, in a ball  $B_R$

$$\mathbf{x} \neq 0 \Rightarrow V(\mathbf{x}) > 0$$

If  $V(\mathbf{0}) = 0$  and the above property holds over the whole state space, then  $V(\mathbf{x})$  is said to be globally positive definite.

**Definition B.7.** If, in a ball  $B_R$ , the function  $V(\mathbf{x})$  is positive definite and has continuous partial derivatives, and if its time derivative along any state trajectory of

system  $\dot{\mathbf{x}} = \mathbf{f}(\mathbf{x})$  is negative semi-definite, i.e.,

$$\dot{V}(\mathbf{x}) \leq 0$$

then  $V(\mathbf{x})$  is said to be a Lyapunov function for the system  $\dot{\mathbf{x}} = \mathbf{f}(\mathbf{x})$ .

**Theorem B.8.** *If, in a ball  $B_R$ , there exists a scalar function  $V(\mathbf{x})$  with continuous first partial derivatives such that*

- $V(\mathbf{x})$  is positive definite (locally in  $B_R$ )
- $\dot{V}(\mathbf{x})$  is negative semi-definite (locally in  $B_R$ )

*then the equilibrium point  $\mathbf{x}^*$  is stable. If, actually, the derivative  $\dot{V}(\mathbf{x})$  is locally negative definite in  $B_R$ , then the stability is asymptotic.*

**Theorem B.9.** *Assume that there exists a scalar function  $V(\mathbf{x})$ , with continuous first order derivatives such that*

- $V(\mathbf{x})$  is positive definite
- $\dot{V}(\mathbf{x})$  is negative definite
- $V(\mathbf{x}) \rightarrow \infty$  as  $\|\mathbf{x}\| \rightarrow \infty$

*then the equilibrium is globally asymptotically stable.*

## APPENDIX C: FLOQUET STABILITY THEORY

Here we first present the concepts on the stability of periodic orbits of linear continuous-time dynamical systems based on the Floquet theory and then show how these results are applied to the local stability of periodic orbits of nonlinear continuous-time dynamical systems.

Let us consider a linear continuous-time dynamical system described by the differential equation

$$\dot{\mathbf{x}}(t) = \mathbf{A}(t)\mathbf{x}(t) \tag{C.1}$$

Assume that  $\mathbf{A}(t)$  is a periodic state matrix of period  $T$  that satisfies

$$\mathbf{A}(t) = \mathbf{A}(t + T), \quad T \in \mathbf{R}, \quad \forall t. \tag{C.2}$$

According to the Floquet theory, the stability of linear periodic systems depends on the eigenvalues of the monodromy matrix, called the *Floquet characteristic multipliers*  $\mu_i$ .

**Proposition C.1.** *(adapted from Theorems 4.1 and 4.2 in [35]) (i) The system (C.1) is asymptotically stable if and only if the characteristic multipliers of  $\mathbf{A}(t)$  have absolute value smaller than 1. (ii) The system (C.1) is stable if and only if the characteristic multipliers of  $\mathbf{A}(t)$  have absolute value smaller than or equal to 1 and those characteristic multipliers with unit-modulus are simple roots of the minimal polynomial of the monodromy matrix  $\Psi(t)$ .*

See Appendix B for stability definitions.

The state transition matrix  $\Phi(t, t_0)$ ,  $t, t_0 \in \mathbf{R}$  of (C.1) is calculated according to the

fundamental matrix definition as follows

$$\begin{aligned}\dot{\Phi}(t, t_0) &= \mathbf{A}(t)\Phi(t, t_0) \\ \Phi(t, t_0) &= \mathbf{I}_n\end{aligned}\tag{C.3}$$

The *monodromy matrix*  $\Psi(t)$  is the transition matrix over a period  $[t, t + T]$ :

$$\Psi(t) = \Phi(t + T, t)\tag{C.4}$$

and thus any solution of (C.1) also satisfies:

$$\mathbf{x}(t + T) = \Phi(t)\mathbf{x}(t)\tag{C.5}$$

Note that  $\Phi(t)$  is a periodic matrix with period  $T$ , but the characteristic multipliers are constant for all  $t$ . The Floquet theory can be used to analyse the stability of periodic orbits of nonlinear systems by studying the convergence of a perturbation, governed by a linearization in the vicinity of the periodic orbit.

Once the equation that governs the perturbation is obtained it is possible to define a continuous-time monodromy matrix  $\Psi(t) \in \mathbf{R}^{n \times n}$  related to the periodic orbit  $\mathbf{x}^*(t)$ :

$$\delta\mathbf{x}(t + T) = \Psi(t)\delta\mathbf{x}(t)\tag{C.6}$$

According to (C.3) and (C.4), the eigenvalues of the monodromy matrix  $\Psi(t)$  are calculated to analyse the stability of the linearized system.

Basically, the linearized system in the closed vicinity of the periodic orbit is described by a linear time-periodic system, then the stabilization of periodic orbits of non-linear system is reduced to stabilization of this type of linear system. Thus, Floquet theory was shown that these linear systems can be stabilized via eigenvalues assignment using state feedback control methods.